

The effects of TiO_2 phase and SiO_2 supports on methyl oleate epoxidation.



Miss Nichaphat Sangkanchanavanich

จุฬาลงกรณ์มหาวิทยาลัย
CHULALONGKORN UNIVERSITY

A Thesis Submitted in Partial Fulfillment of the Requirements
for the Degree of Master of Engineering in Chemical Engineering

Department of Chemical Engineering

Faculty of Engineering

Chulalongkorn University

Academic Year 2018

Copyright of Chulalongkorn University

ผลของเฟสของไททานเนียม ไดออกไซด์ และตัวรองรับ ซิลิกอนไดออกไซด์ ที่มีผลต่อปฏิกิริยา อิพอก
ซีเดชัน ของเมทิล โอลิเอต



วิทยานิพนธ์นี้เป็นส่วนหนึ่งของการศึกษาตามหลักสูตรปริญญาวิศวกรรมศาสตรมหาบัณฑิต
สาขาวิชาวิศวกรรมเคมี ภาควิชาวิศวกรรมเคมี
คณะวิศวกรรมศาสตร์ จุฬาลงกรณ์มหาวิทยาลัย
ปีการศึกษา 2561
ลิขสิทธิ์ของจุฬาลงกรณ์มหาวิทยาลัย

Thesis Title The effects of TiO₂ phase and SiO₂ supports on methyl
oleate epoxidation.
By Miss Nichaphat Sangkanchanavanich
Field of Study Chemical Engineering
Thesis Advisor Professor Piyasan Prasertthdam, Ph.D.
Thesis Co Advisor Wipark Anutrasakda, Ph.D.

Accepted by the Faculty of Engineering, Chulalongkorn University in Partial
Fulfillment of the Requirement for the Master of Engineering

..... Dean of the Faculty of Engineering
(Associate Professor Supot Teachavorasinskun, Ph.D.)

THESIS COMMITTEE

..... Chairman
(Associate Professor Deacha Chatsiriwech, Ph.D.)

..... Thesis Advisor
(Professor Piyasan Prasertthdam, Ph.D.)

..... Thesis Co-Advisor
(Wipark Anutrasakda, Ph.D.)

..... Examiner
(Professor Joongjai Panpranot, Ph.D.)

..... External Examiner
(Nilubon Jonganurakkun, Ph.D.)

นิพนธ์ แสงกาญจนวนิช : ผลของเฟสของไททาเนียม ไดออกไซด์ และตัวรองรับ ซิลิกอนไดออกไซด์ ที่มีผลต่อปฏิกิริยา อีพอกซิเดชัน ของเมทิล โอลิเอต. (The effects of TiO_2 phase and SiO_2 supports on methyl oleate epoxidation.) อ.ที่ปรึกษาหลัก : ศ. ดร.ปิยะสาร ประเสริฐธรรม, อ.ที่ปรึกษาร่วม : อ. ดร.วิภาค อนุตรศักดิ์

งานวิจัยนี้ศึกษาเรื่องปฏิกิริยาอีพอกซิเดชันของเมทิลโอลิเอตกับไททาเนียม ไดออกไซด์หรือไททาเนียม ไดออกไซด์บนตัวรองรับซิลิกอนไดออกไซด์กับไฮโดรเจนเปอร์ออกไซด์ การศึกษาของตัวเร่งปฏิกิริยาชนิดไททาเนียม ไดออกไซด์สนใจไททาเนียม ไดออกไซด์จากอุตสาหกรรมและสังเคราะห์จากวิธีโซลเจล ความสามารถในการเร่งปฏิกิริยาและความสามารถในการเลือกเกิดของตัวเร่งจากอุตสาหกรรมมีค่าสูงที่สุดคือ ไททาเนียม ไดออกไซด์ชนิด บี ซึ่งให้ค่าอยู่ที่ร้อยละ 46.10 และร้อยละ 79.75 ตามลำดับ สำหรับสังเคราะห์ด้วยวิธีโซลเจลตัวเร่งปฏิกิริยาที่ให้ค่าสูงที่สุดคือการเผาที่อุณหภูมิ 300 องศาให้ความสามารถในการเร่งปฏิกิริยาอยู่ที่ร้อยละ 75.82 และความสามารถในการเลือกเกิดอยู่ที่ 90.85 เนื่องจากความเป็นผลึกที่ต่ำและพื้นที่ผิวที่มาก ซิลิกอนไดออกไซด์ต่างชนิดกัน แสดงค่าความสามารถในการเร่งปฏิกิริยาและความสามารถในการเลือกเกิดที่ต่างกัน ซิลิกาไลที่มีความสามารถในการเร่งปฏิกิริยาสูงที่สุดโดยมีค่าร้อยละ 44.41 ตัวรองรับเอสบีเอ 15 มีความสามารถในการเลือกเกิดสูงที่สุดโดยมีค่าร้อยละ 58.90 การสังเคราะห์ที่ต่างกันแสดงความสามารถในการเร่งปฏิกิริยาที่เท่ากันที่ค่าประมาณร้อยละ 35 อย่างไรก็ตามการฝังตัวแบบเปียกให้ค่าการเลือกเกิดที่ร้อยละ 28.43 ซึ่งมากกว่าวิธีสังเคราะห์แบบอื่น ไททาเนียมที่ต่างกันให้ผลว่าเมื่อ ไททาเนียมมากขึ้นความสามารถในการเร่งปฏิกิริยาจะมากขึ้นแต่ความสามารถในการเลือกเกิดจะน้อยลงโดยเพิ่มไททาเนียมจากร้อยละ 1.5 ถึงร้อยละ 15 ความสามารถในการทำปฏิกิริยาเพิ่มจากร้อยละ 18.86 เป็นร้อยละ 97.49 และความสามารถในการเลือกเกิดลดลงจากร้อยละ 42.44 เป็น 0

สาขาวิชา	วิศวกรรมเคมี	ลายมือชื่อนิสิต
	
ปี	2561	ลายมือชื่อ อ.ที่ปรึกษาหลัก
การศึกษา	
		ลายมือชื่อ อ.ที่ปรึกษาร่วม
	

6070190721 : MAJOR CHEMICAL ENGINEERING

KEYWORD: epoxidation of methyl oleate; epoxide methyl oleate; TiO₂/SiO₂; TiO₂
by sol-gel; crystallinity; silanol group

Nichaphat Sangkanchanavanich : The effects of TiO₂ phase and SiO₂ supports on methyl oleate epoxidation.. Advisor: Prof. Piyasan Praserttham, Ph.D. Co-advisor: Wipark Anutrasakda, Ph.D.

This work studies about the epoxidation reaction of methyl oleate with TiO₂ or TiO₂/SiO₂ catalysts and hydrogen peroxide. Study of TiO₂ catalysts interests in catalysts from commercial and sol gel method. The highest catalytic activity and selectivity of TiO₂ from commercial is TiO₂ commercial type B which gives 46.10% and 79.75%, respectively. For sol gel method, the highest catalytic activity at 75.82% and selectivity at 90.85% is TiO₂ calcination temperature at 300OC, due to low crystallinity and high surface area. TiO₂/ SiO₂ with different type of SiO₂ support (MCM-41, SBA-15, silicalite, silica gel and fumed silica) shows different catalytic activity and selectivity. The highest catalytic activity is TiO₂/Silicalite with 44.41% conversin. The highest selectivity is TiO₂/SBA-15 with 58.90% selectivity. TiO₂/SiO₂ by different synthesis method (wet impregnation, grafting and incipient wetness impregnation) show the same catalytic activity around 35% . However, wet impregnation method gave higher selectivity at 28.43% than other synthesis method. TiO₂/SiO₂ with different Ti loading show that the more Ti loading give more catalytic activity but less selectivity of epoxidation reaction. Which increase Ti from 1.5% to 15% catalytic activity increase from 18.86% to 97.49% and selectivity decrease from 42.44% to 0.00% selectivity.

Field of Study: Chemical Engineering

Student's Signature

.....

Academic 2018

Advisor's Signature

Year:

.....

Co-advisor's Signature

.....

ACKNOWLEDGEMENTS

I would like to express my sincere gratitude toward my advisor, Professor Piyasan Prasertthdam, Ph.D. and my co- advisor, Wipark Anutrasakda, Ph.D for the continuous advice and guidance in order to solve the problem in this research as well as invaluable help, understanding and continued support. This thesis would not be completely achieved without their advice.

Furthermore, I would like to appreciate for every suggestion and critique from Associate Professor Deacha Chatsiriwech, Ph. D, as a chairman, Professor Joongjai Panpranot, Ph.D, and Dr. Nilubon Jongsurakun, Ph.D as the members of the thesis committee, who devoted their valuable time to review this thesis.

Additionally, I would like to show my wholeheartedly gratitude for financial support from the Global Green Chemical Public Company Limited (GGC) and CAT-REAC industrial project (RDG6150012).

Last but not least, I would like to show my appreciation for all supports and carefulness from my beloved family and friends who are in the Center of Excellence on Catalysis and Catalytic Reaction Engineering laboratory. As, this thesis would unlikely be successful without their supports.

จุฬาลงกรณ์มหาวิทยาลัย
CHULALONGKORN UNIVERSITY

Nichaphat Sangkanchanavanich

TABLE OF CONTENTS

	Page
ABSTRACT (THAI).....	iii
ABSTRACT (ENGLISH)	iv
ACKNOWLEDGEMENTS	v
TABLE OF CONTENTS.....	vi
LIST OF TABLES	x
LIST OF FIGURES	xii
CHAPTER I INTRODUCTION.....	1
1.1. Introduction.....	1
1.2. Objective.....	3
1.3. Scope of research	3
1.4 Research methodology	4
CHAPTER II BACKGROUND AND LITERATURE REVIEWS.....	6
2.1. Epoxidation reaction of methyl oleate.....	6
2.1.1. Prileshajew reaction	8
2.1.2. Side reaction of epoxidation	9
2.1.3. Effect of temperature	10
2.1.4. Effect of solvent.....	11
2.1.5 Effect of reaction time	13
2.2. TiO ₂	13
2.3. TiO ₂ /SiO ₂	16
2.4. Other catalyst for epoxidation reaction	22

CHAPTER III EXPERIMENTAL	24
3.1. Materials and chemicals.....	24
3.2. Preparation of catalyst.....	25
3.2.1 Synthesis of TiO ₂ by sol-gel method.....	25
3.2.2 Synthesis of TiO ₂ with SiO ₂ supported by incipient wetness impregnation method	25
3.2.3 synthesis of TiO ₂ /fumed SiO ₂ by incipient wetness impregnation method .	25
3.2.4 Synthesis of TiO ₂ /fumed SiO ₂ by wet impregnation method.....	26
3.2.5 Synthesis of TiO ₂ /fumed SiO ₂ by grafting method.....	26
3.2.6 Synthesis of TiO ₂ / fumed SiO ₂ with different Ti loading by incipient wetness impregnation method.....	26
3.3. Catalyst characterization techniques.....	27
3.3.1. N ₂ -physisorption.....	27
3.3.2. Scanning electron microscope (SEM) and energy dispersive X-ray spectroscopy (EDX).....	27
3.3.3. X-ray Diffraction (XRD).....	27
3.3.4. UV-visible spectroscopic analysis (UV-vis)	28
3.3.5 Fourier transform infrared spectroscopy (FT-IR).....	28
3.3.6 X-ray photoelectron spectroscopy (XPS).....	28
3.3.7 Thermogravimetric analysis (TGA)	28
3.4 Catalytic activity on epoxidation reaction	28
3.4.1. Epoxidation reaction.....	28
3.4.2. Reaction products analyzed.....	29
CHAPTER IV RESULTS AND DISCUSSION.....	31

4.1. Epoxidation of TiO ₂ catalysts with different calcination temperatures	31
4.1.1. Catalytic activity and selectivity of TiO ₂ catalyst	31
4.1.2. Characterization of TiO ₂ catalyst	33
4.2. Epoxidation of TiO ₂ /SiO ₂ catalysts with different SiO ₂ supported	40
4.2.1. Catalytic activity and selectivity of TiO ₂ /SiO ₂ catalyst with different SiO ₂ supported.	40
4.2.2. Characterization of TiO ₂ /SiO ₂ catalyst with different SiO ₂ supported.....	41
4.3. Epoxidation of TiO ₂ /SiO ₂ catalysts by different synthesis method	50
4.3.1. Catalytic activity and selectivity of TiO ₂ /SiO ₂ catalysts by different synthesis method.	50
4.3.2. Characterization of TiO ₂ /SiO ₂ by different synthesis method	51
4.4. Epoxidation of TiO ₂ /SiO ₂ catalysts with different %Ti loading.....	55
4.4.1. Catalytic activity and selectivity of TiO ₂ /SiO ₂ catalysts with different %Ti loading	55
4.4.2. Characterization of TiO ₂ /SiO ₂ catalysts with different %Ti loading	58
CHAPTER V CONCLUSIONS AND RECOMMENDATIONS.....	61
5.1 Conclusions	61
5.2 Recommendations	62
REFERENCES	63
APPENDICES.....	69
APPENDICES A: CALCULATION OF CRYSTALLITE SIZE	69
Calculation of the crystallite size by Debye-Scherrer equation.....	69
APPENDICES B: CALCULATION OF WEIGHT FRACTION OF ANATASE, RUTILE AND BROOKITE PHASE OF TiO ₂	71

Calculation of the weight fraction	71
APPENDICES C: CALCULATION OF CATALYST PREPARATION	73
For TiO ₂ / fumed SiO ₂ by incipient wetness impregnation	73
VITA	74



LIST OF TABLES

	Page
Table 1 composition of biodiesel from vegetable oil.	6
Table 2 Physical properties of methyl oleate.	6
Table 3 Physical properties of methyl oleate epoxide.	8
Table 4 Effect of Temperature on Epoxidation of methyl oleate.	10
Table 5 Influence of the solvent on the initial rate of reaction, conversion of methyl oleate X_{MO} , selectivity SME and conversion of hydrogen peroxide $X_{H_2O_2}$ in the epoxidation of methyl oleate over TS-1 (Ind.) at 323 K after 24 h.	12
Table 6 Physical properties of acetonitrile.	12
Table 7 Physical properties of hydrogen peroxide.	12
Table 8 Physical properties of TiO_2	14
Table 9 Catalytic Activity of TiO_2/SiO_2 catalysts with Different TiO_2 Loadings.	18
Table 10 Effect of Calcination Temperature on Catalytic Properties of TiO_2/SiO_2	19
Table 11 Other catalysts for epoxidation reaction.	22
Table 12 Chemicals used in catalyst preparation.	24
Table 13 Chemicals used in epoxidation reaction.	24
Table 14 list of substrate solution.	29
Table 15 list of gas chromatography condition.	30
Table 16 Crystallite size, Anatase weight fraction and %crystalline of TiO_2 catalysts.	34
Table 17 H_2O adsorbed by Thermal gravimetric analysis (TGA).	42
Table 18 Conversion of TiO_2/SiO_2 catalyst and composition of each TiO_2 species at catalyst surface.	43

Table 19 Effect of pore size and Wt% H ₂ O adsorbed to selectivity of TiO ₂ /SiO ₂ support.	48
Table 20 Wt% of Ti on TiO ₂ /SiO ₂ surface from SEM-EDX analysis and surface area from N ₂ physisorption analysis.....	53



LIST OF FIGURES

	Page
Figure 1 epoxidation reaction of methyl oleate.	7
Figure 2 path way of epoxidation reaction.	7
Figure 3 Prileshajew reaction.....	9
Figure 4 Side reaction for the epoxidation of methyl oleate with H ₂ O ₂	10
Figure 5 Effect of reaction temperature on conversion of methyl oleate XMO and epoxide selectivity SME in the epoxidation of methyl oleate over TS-1.	11
Figure 6 Conversion and selectivity as a function of time of methyl oleate epoxide.	13
Figure 7 TiO ₂ crystal structures: rutile (a), anatase (b) and brookite (c). Ti ⁴⁺ sits at the center of the octahedron and O ₂ at each corner.....	14
Figure 8 Mechanism of inactivation of amorphous titanasilicate epoxidation catalysts in presence of water.	16
Figure 9 Surface hydroxyl group of TiO ₂ /Silicalite.	17
Figure 10 Surface hydroxyl group of TiO ₂ /SBA-15.	17
Figure 11 XRD patterns of TiO ₂ /SiO ₂ catalysts with different TiO ₂ loadings: (a) support; (b) 1%; (c) 5%; (d) 10%; (e) 12%; (f) 14%; (g) 16%; (h) 20%; and (i) nano anatase TiO ₂	18
Figure 12 XRD spectra of 12 wt% TiO ₂ /SiO ₂ catalysts under different calcination temperature: (a) 300°C; (b) 400°C; (c) 500°C; (d) 550°C; (e) 600°C; (f) 700°C; and (g) 800°C.....	19
Figure 13 FTIR spectra of samples.....	20
Figure 14 FTIR region in absorbance mode: (a) SBA-15; (b) 40Ti-SBA-iso; (c) 20Ti-SBA-iso; (d) 40Ti-SBA-P25 and (e) 20Ti-SBAP25.	20

Figure 15 XPS spectra of Ag-Ti nanotubes after self-doped Ti^{3+}	21
Figure 16 UV/vis spectra of the Ti-MCM-41 catalysts with different molar ratios of Si:Ti in the crystallization gel (respectively, 40:1, 30:1, 20:1, and 10:1).....	21
Figure 17 Conversion of all TiO_2 catalysts in epoxidation of methyl oleate at 5 h.	32
Figure 18 Selectivity of all TiO_2 catalyst in epoxidation of methyl oleate at 5 h.....	32
Figure 19 X-ray diffraction pattern of all TiO_2 catalysts prepared by sol-gel method and commercial TiO_2	35
Figure 20 Fourier transform infrared spectroscopy (FT-IR) of all TiO_2 catalysts prepared by sol-gel method.	36
Figure 21 Thermal gravimetric analysis (TGA) of gel TiO_2 (TiO_2 catalyst before calcination).	37
Figure 22 %Conversion with surface area and %crystalline of TiO_2 catalysts.	37
Figure 23 %Selectivity with surface area and %crystalline of TiO_2 catalysts.	38
Figure 24 %Conversion of TiO_2 catalyst calcination at $300^\circ C$ as a function of time.....	38
Figure 25 Conversion of reuse TiO_2 catalyst calcination temperature at $300^\circ C$ at 5 h...	39
Figure 26 Selectivity of reuse TiO_2 catalyst calcination temperature at $300^\circ C$ at 5 h....	39
Figure 27 Catalytic activity of all TiO_2/SiO_2 catalysts in epoxidation of methyl oleate. ...	40
Figure 28 Selectivity of all TiO_2/SiO_2 catalyst in epoxidation of methyl oleate at 5 h.	41
Figure 29 Thermal gravimetric analysis (TGA) of TiO_2/SiO_2 with different support.....	42
Figure 30 Scanning electron microscopy (SEM) and Energy dispersive x-ray spectroscopy (EDX) results of TiO_2/SiO_2 catalyst.....	44
Figure 31 X-ray diffraction (XRD) of TiO_2/SiO_2 catalysts.....	45
Figure 32 Fourier transform infrared spectroscopy (FT-IR) of TiO_2/SiO_2 with different SiO_2 support.....	45

Figure 33 X-ray photoelectron spectroscopy (XPS) of TiO ₂ /SiO ₂ with different support.	46
Figure 34 N ₂ physisorption of TiO ₂ with different SiO ₂ supports	48
Figure 35 UV-vis of TiO ₂ with different SiO ₂ supports	49
Figure 36 wt% H ₂ O adsorbed and selectivity of all catalysts	49
Figure 37 Catalytic activity of TiO ₂ /SiO ₂ different synthesis methods.	51
Figure 38 Selectivity of TiO ₂ /SiO ₂ different synthesis methods.	52
Figure 39 SEM micrographs of A) fumed silica support, B) TiO ₂ /SiO ₂ by incipient wetness impregnation, C) TiO ₂ /SiO ₂ by grafting and D) TiO ₂ /SiO ₂ by wet impregnation.	53
Figure 40 X-ray diffraction patterns of TiO ₂ /SiO ₂ by wet impregnation, incipient wetness impregnation and grafting method.	54
Figure 41 UV-Vis spectra of TiO ₂ /SiO ₂ by wet impregnation, incipient wetness impregnation and grafting method.	55
Figure 42 Catalytic activity of TiO ₂ /SiO ₂ catalysts with different %Ti loading.	56
Figure 43 Selectivity of TiO ₂ /SiO ₂ catalysts with different %Ti loading.....	57
Figure 44 Conversion of TiO ₂ /SiO ₂ catalysts with different %Ti loading.....	57
Figure 45 Selectivity of TiO ₂ /SiO ₂ catalysts with different %Ti loading.....	58
Figure 46 X-ray diffraction (XRD) of TiO ₂ /SiO ₂ catalysts with different %Ti loading.....	59
Figure 47 Fourier transform infrared spectroscopy (FT-IR) of TiO ₂ /SiO ₂ with different %Ti loading.....	60

CHAPTER I

INTRODUCTION

1.1. Introduction

Palm is one of the most abundant agricultural goods in Thailand. In the south of Thailand, although rubber is the first in amount, the second most are palm. The problem is that nowadays palm is overstocked. Thus, its price is extremely low. Therefore, palm is changed into biodiesel, which will increase palm selling price. However, we cannot use more than B5 (B5 is 5% biodiesel and 95% diesel.) because of mechanical problems. In the past, we use B5 and nowadays we use B3 which uses less biodiesel. So, biodiesel is overstocked. Consequently, its price is extremely low. Therefore, this project's purpose is to raise the value of biodiesel from palm.

The largest share of renewables in the industry is fat and oils. Thus, the development of renewable raw materials is likely to be an important issue. Furthermore, fat and oils of vegetable and animal can be converted to fatty acid methyl ester (FAMES) for biodiesel. Vegetable oils and their FAMES are large scale, biodegradable, eco-friendly, low toxicity and inexpensive. The largest scale of biodiesel is from palm oil and the major compositions derived from palm oil is methyl oleate (C18:1) [1-5]. In the present, biodiesel is overpriced due to the large scale and low demand for biodiesel. On the other hand, electrical energy has played an important role as a renewable energy in this industry such as the car industry. Also, the electrical energy has been investigated in many types of research because this is an eco-friendly and cleaner energy. Therefore, the study of high-value product from biodiesel is widely studied (i.e., hydrogenation, ozone cleavage, and epoxidation). Biodiesel mostly consists of unsaturated fatty acid methyl ester, so epoxidation reaction is interesting. Epoxidation reaction converts the unsaturated double bonds fatty acid methyl ester to oxirane ring or epoxide. Epoxide of fatty acid derivatives from vegetable oils are used in large scale application [5-8] such as plasticizers [3] and stabilizer in PVC, intermediates in polyurethane polyols [9], components for lubricants [10], cosmetics, polymer precursors for the preparation of

various polymers [11], wood impregnation, biofuel additives[12] and pharmaceuticals [1].

In industrial scale, epoxidation reaction is performed by the Prileshajew reaction, a homogeneous reaction using soluble mineral acids such as H_3PO_4 , HCl or H_2SO_4 as catalysts. The peracid will attack the double bonds then form the oxirane ring. The Prileshajew reaction is widely used as PVC plasticizer and intermediates. The Prileshajew reaction uses per carboxylic acid such as peracetic or performic with hydrogen peroxide as an oxidant. Hydrogen peroxide promotes the formation of peracetic acid [2, 7, 12, 13]. However, there are problems concerning this reaction. Firstly, Peracids and highly concentrated hydrogen peroxide are toxic. On the other contrary, hydrogen peroxide produces only water as a by-product. Therefore, hydrogen peroxide is commonly used [14, 15]. Secondly, C1-C3 carboxylic acids are corrosive. Thirdly, the homogeneous reaction is difficult for catalyst separation and low selectivity. A side reaction is the oxirane ring opening due to the acidic reaction. According to **Figure 4**, the side reactions of epoxidation are ring opening, oxidative cleavage, and rearrangement. [2, 11-13, 16].

Those problems from Prileshajew reaction can eliminate by using a heterogeneous catalyst. Heterogeneous catalysts are easy to separate, reuse and give high selectivity. Heterogeneous catalysts have been reported for epoxidation reaction such as acidic resin, metal oxides, Ti-silicas, Nd(v) -silica, Sulfated- SnO_2 and polyoxometalate [2, 5, 8, 10, 12]. Over the past decade, metal oxide catalyst has been widely developed with the structure of microporous and mesoporous materials. According to the broad modification such as calcination temperature, metal loading and supported material of metal oxides. Many metal ions have been reported such as rhenium, molybdenum, titanium, vanadium, chromium, and tungsten as catalysts [15, 17-19]. Titanium-silica catalysts have been widely studied according to high conversion, selectivity, and recoverability [6]. Titanium dioxide has been generally used in many reactions such as photocatalytic reaction, selective catalytic reduction, transesterification and epoxidation reaction [20]. Silica supported presence high

dispersion for metal oxide. Silica surface is fairly inert and hydrophilic [21]. Mostly, TiO_2 - SiO_2 , Ti-MCM-41, and TS-1 are used as catalysts [2, 4, 8, 16].

This project focuses on heterogeneously catalyzed epoxidation of methyl oleate with hydrogen peroxide as oxidant, acetonitrile as solvent at constant temperature and pressure. Study in catalytic activity, the selectivity of TiO_2 and TiO_2 with different SiO_2 supported.

1.2. Objective

To investigate the effects of different SiO_2 supports of TiO_2 catalysts on epoxidation reaction.

1.3. Scope of research

Effect of TiO_2 phase and SiO_2 supported with epoxidation reaction of methyl oleate with hydrogen peroxide as oxidant. Acetonitrile is used as a solvent. The reaction temperature is 50°C .

1.3.1. Synthesis of different crystallinity of TiO_2 from various calcination temperatures (100°C , 200°C , 300°C , 400°C , and 500°C) by sol-gel method.

1.3.2. Synthesis of TiO_2 with different SiO_2 type (MCM-41, SBA-15, silicalite, silica-gel, and fumed silica) via incipient wetness impregnation method.

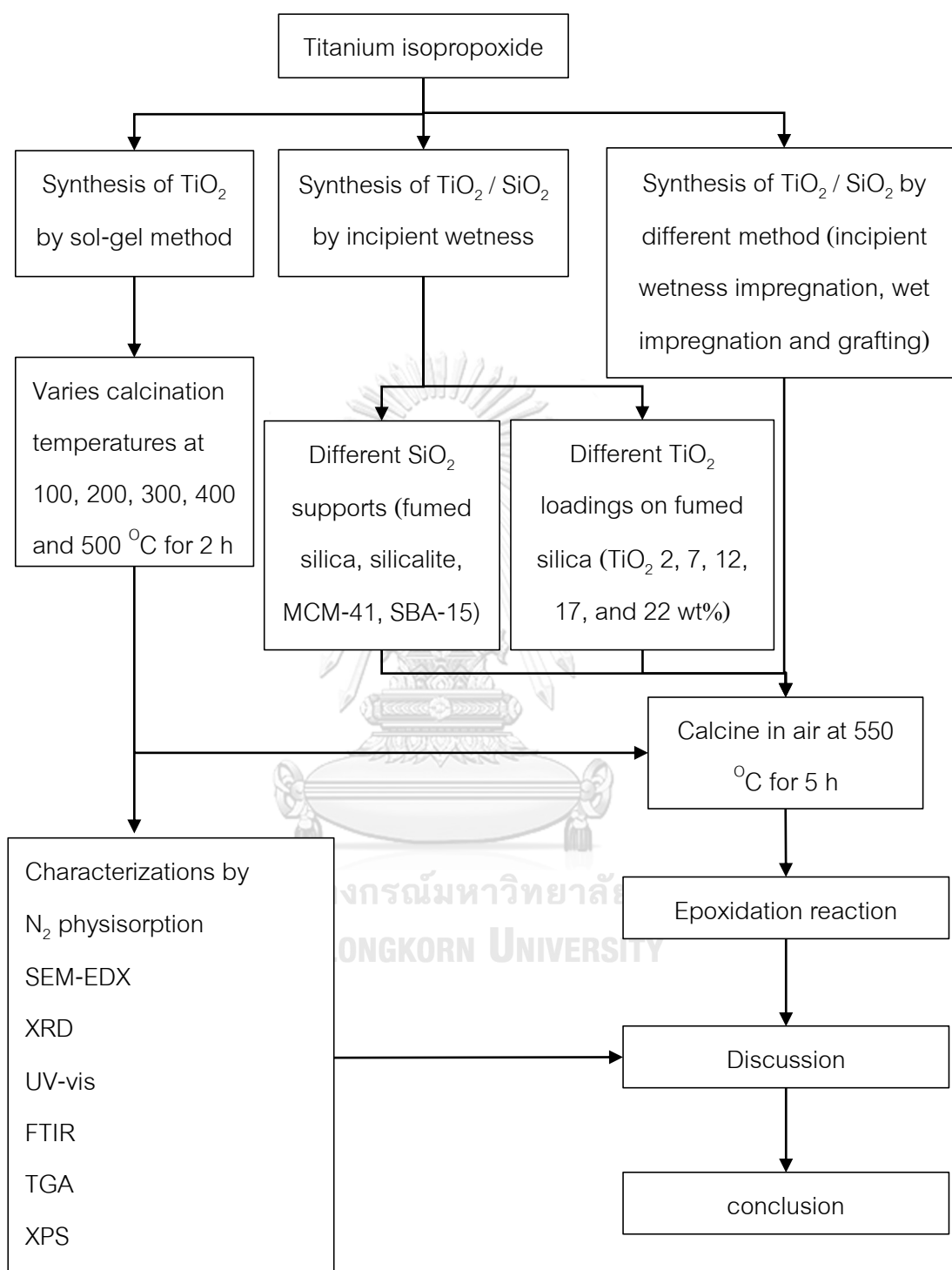
1.3.3. Synthesis of TiO_2 /fumed SiO_2 by different synthesis methods (incipient wetness impregnation, wet impregnation, and grafting).

1.3.4. Synthesis of TiO_2 /fumed SiO_2 with different TiO_2 loadings (1.5%, 2.5%, 3.2%, 4.0%, 4.7%, 10%, and 15%) via incipient wetness impregnation method.

1.3.5. Characterization of the catalysts by N_2 -physisorption, SEM-EDX, XRD, UV-vis, TGA, FTIR and XPS.

1.3.6. Catalytic activity and selectivity of epoxidation reaction were investigated by GC-MS column DB-5

1.4 Research methodology



Then the thesis is arranged as follows:

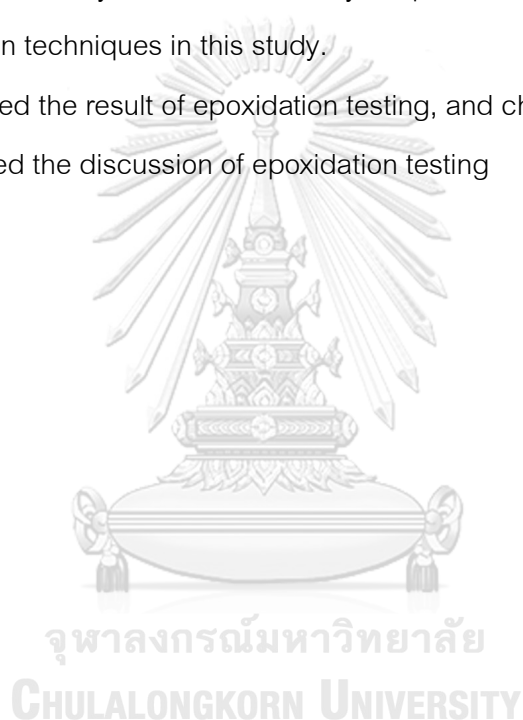
Chapter I presented the motivation of the research, the research objective, the research scopes, and the research methodology.

Chapter II presented the theory and literature reviews of epoxidation reaction and basic knowledge of physical and chemical properties of reactant (methyl oleate), solvent (acetonitrile), oxidant (Hydrogen peroxide) and products (methyl oleate epoxide) including their application.

Chapter III presented the synthesis of the catalyst, epoxidation of methyl oleate testing, and characterization techniques in this study.

Chapter IV presented the result of epoxidation testing, and characterization techniques.

Chapter V presented the discussion of epoxidation testing



CHAPTER II

BACKGROUND AND LITERATURE REVIEWS

This chapter is undertaken to review the fundamental concept and literature based on past researches. The first section of the chapter will investigate the general information about the epoxidation reaction of methyl oleate. Then, the following section will explain about TiO_2 . Finally, the last section will describe about TiO_2 with SiO_2 supported.

2.1. Epoxidation reaction of methyl oleate

Oils and fats of vegetable are the most interesting renewable feedstock. Oils and fats can be converted to fatty acid methyl ester (FAMES) by transesterification. According to Table 1, the most component of FAMES from palm is methyl oleate ($\text{C}_{19}\text{H}_{36}\text{O}_2$), which consist of one double bond. Physical properties of methyl oleate are listed in Table 2. This FAMES or biodiesel can be upgraded to the high-value product such as epoxide, fatty alcohol, methyl ester sulfonate, and biowax. Heterogenous epoxidation reaction is the most interesting reaction, due to mild condition reaction, acid-free reaction and easy to remove the catalyst.

Table 1 composition of biodiesel from vegetable oil. [22]

Fatty acid		Palm	Olive	Peanut	Rape	Soybean	Sunflower	Grape	H.O. Sunflower	Almond	Corn
Lauric	C12:0	0.1	0.0	0.0	0.0	0.0	0.0	0.0	0.0	0.0	0.0
Myristic	C14:0	0.7	0.0	0.1	0.0	0.0	0.0	0.1	0.0	0.0	0.0
Palmitic	C16:0	36.7	11.6	8.0	4.9	11.3	6.2	6.9	4.6	10.4	6.5
Palmitoleic	C16:1	0.1	1.0	0.0	0.0	0.1	0.1	0.1	0.1	0.5	0.6
Stearic	C18:0	6.6	3.1	1.8	1.6	3.6	3.7	4.0	3.4	2.9	1.4
Oleic	C18:1	46.1	75.0	53.3	33.0	24.9	25.2	19.0	62.8	77.1	65.6
Linoleic	C18:2	8.6	7.8	28.4	20.4	53.0	63.1	69.1	27.5	7.6	25.2
Linolenic	C18:3	0.3	0.6	0.3	7.9	6.1	0.2	0.3	0.1	0.8	0.1
Arachidic	C20:0	0.4	0.3	0.9	0.0	0.3	0.3	0.3	0.3	0.3	0.1
Gadoleic	C20:1	0.2	0.0	2.4	9.3	0.3	0.2	0.0	0.0	0.0	0.1
Behenic	C22:0	0.1	0.1	3.0	0.0	0.0	0.7	0.0	0.7	0.1	0.0
Erucic	C22:1	0.0	0.0	0.0	23.0	0.3	0.1	0.0	0.0	0.0	0.1
Lignoceric	C24:0	0.1	0.5	1.8	0.0	0.1	0.2	0.0	0.3	0.2	0.1
Nervonic	C24:1	0.0	0.0	0.0	0.0	0.0	0.0	0.0	0.0	0.4	0.0

Table 2 Physical properties of methyl oleate.

Properties	Information
Molecular weight	296.49 g/mol
Density	0.874 g/ml at 20 ^o C
Normal boiling point	218 ^o C
Vapor pressure	10 mmHg (205 ^o C)

According to **Figure 1**, epoxidation reaction converts the double bond to oxirane ring [2]. As shown in **Figure 2**, epoxidation has two path way. The first path way is direct epoxidation. This path way, epoxidation form by Ti-OOH site on the catalyst [14]. The second path way is allylic oxidation. Which epoxidation form by radical of TiO. Epoxidation of methyl oleate converts to methyl oleate epoxide ($C_{19}H_{36}O_3$). Methyl oleate epoxide is also known as Epoxidized methyl oleate, Methyl 3-octyloxiraneoctanoate, Methyl 8- (3-octyloxiranly) octanoate, Methyl 9,10-epoxyoctadecanoate, Methyl 9,10-epoxystearate, Octadecanoic acid, 9,10-epoxy-, methyl ester, 3-Octyloxiraneoctanoic acid methyl ester and Oxiraneoctanoic cid, 3-octyl-, methyl ester. The physical properties of methyl oleate epoxide are listed in **Table 3**.

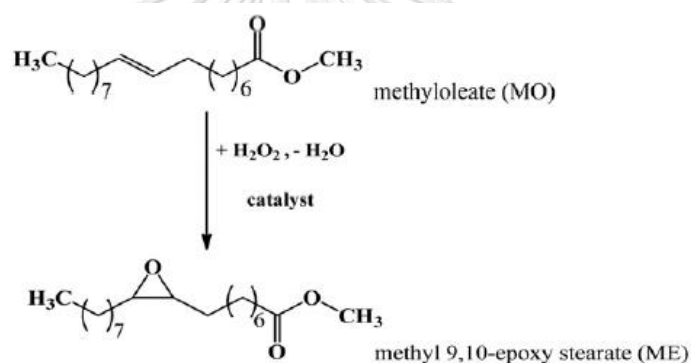


Figure 1 epoxidation reaction of methyl oleate. [2]

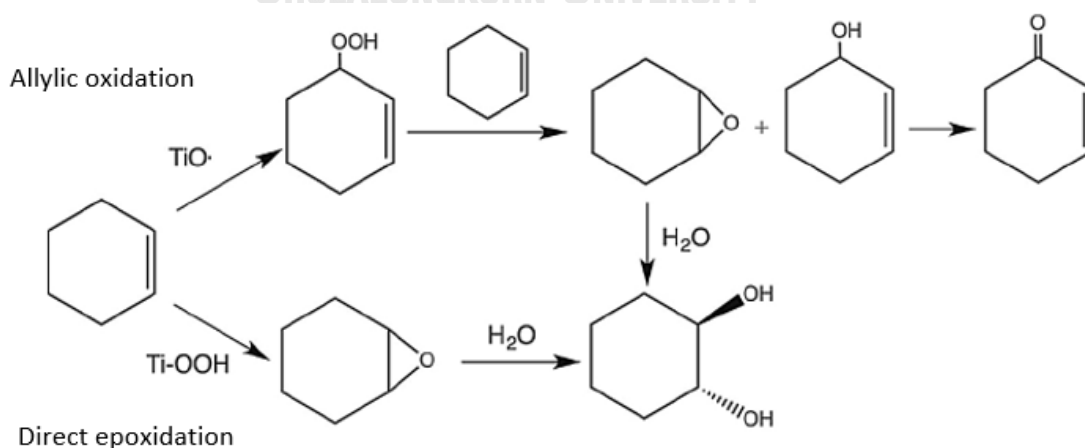


Figure 2 path way of epoxidation reaction. [14]

Table 3 Physical properties of methyl oleate epoxide.

Properties	Information
Molecular weight	312.49 g/mol

Applications of methyl oleate epoxide include the additive for lubricants, intermediates in polymer and plasticizer. Oxirane ring or epoxide can improve oxidation and low temperature properties. Therefore, methyl oleate epoxide uses as an additive for lubricants [10, 23]. Methyl oleate epoxide also uses as intermediates in polymer. It is also an intermediate used to synthesize biobased polyurethane. Ring opening of methyl oleate improves rheological properties of PVC. so it uses as intermediates for bioplasticizer in PVC [24]. The main advantages of methyl oleate epoxide are low diffusion coefficients, low volatility and biodegraded by the microbial agent[3] . Therefore, methyl oleate epoxide is used as plasticizer of polymeric materials.

2.1.1. Prileshajew reaction

In industry, epoxidation reaction is carried out by the prileshajew reaction. The prilshajew reaction is a homogenous reaction. The prilshajew reaction is the eponymous name of Nikolaus Prileshajew who first revealed this reaction in 1909. Prileahajew reaction uses per carboxylic acid such as peracetic and performic and hydrogen peroxide as oxidant. Commonly used acid catalyts such as H_3PO_4 , HCl or H_2SO_4 . According to **Figure 2**, (a) hydrogen peroxide and acetic acid react to give peracetic acid. (b) This peracetic acid reacts with unsaturated fatty acids methyl ester and converts to epoxide. (c) An excess of hydrogen peroxide and acetic acid permit ring opening of epoxide[25]. This reaction is difficult to neutralize or separate the strong acids catalyts. Therefore, it causes a ring opening reaction. New sustainable process based on green reagent and clean technology is important. The first sustainable process is an ion-exchange resin catalyts. Since the resin can be easily separated from the solution. In many epoxidation reactions, yields are low because epoxide converted

to ring opening [26]. Therefore, the heterogeneous catalyst is interesting. Hydrogen peroxide is used as oxidants because it produces only water as the by-product.

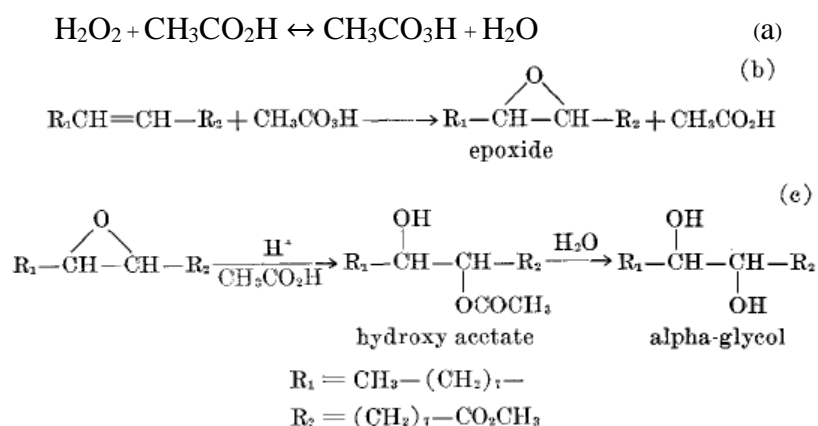
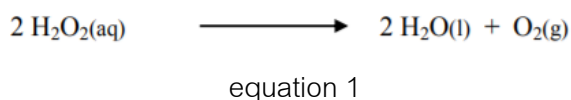


Figure 3 Prileshajew reaction. [25]

2.1.2. Side reaction of epoxidation

According to Figure 3, there are 3 side reaction of the epoxidation reaction, including rearrangement, hydrolysis or ring opening, and oxidative cleavage. Ketones are derived from rearrangement reaction. Both hydrolysis and oxidative cleavage are formed under acidic conditions. Those side reactions expand with increasing reaction time. Nevertheless, the lower epoxidation selectivity is mainly due to hydrolysis reaction [5, 8]. According to equation 1, the decomposition of hydrogen peroxide is one of the results of hydrolysis. The decomposition of hydrogen peroxide is up to 78% in 5 h. This explains the loss of activity along the reaction time. In fact, as long as reaction goes the oxidant are lost and formed water, which is able to produce a ring opening reaction [13]. On the contrary, a small amount of water is necessary to rehydrate the surface of the catalyst.

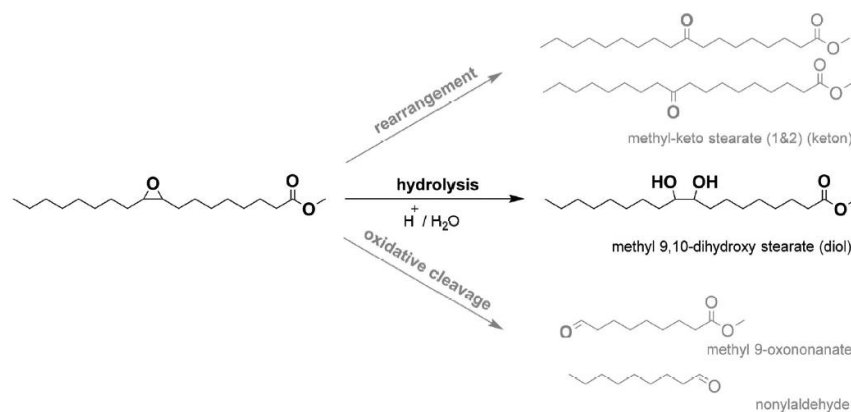


Figure 4 Side reaction for the epoxidation of methyl oleate with H_2O_2 . [8]

2.1.3. Effect of temperature

Temperature has affected on both activity and selectivity. Epoxidation reaction was active at low temperature. According to **Table 4**, increasing temperature activity of epoxidation also increased. A slightly increase in reaction temperature can promote the selectivity of an epoxide. However, the selectivity of epoxide is decreased when the temperature is higher than $25\text{ }^\circ\text{C}$ [12]. According to **Figure 5**, the conversion of epoxidation of methyl oleate is increased with increasing temperature. On the other hand, selectivity is slightly affected by temperature up to $60\text{ }^\circ\text{C}$. At higher temperatures, the formation of by-products also occurs [2]. The optimum reaction temperature of methyl oleate is $50\text{ }^\circ\text{C}$. Both **Table 4** and **Figure 5** showed that different substrates have different optimum reaction temperatures. Therefore, it showed that epoxidation reaction was favored at low temperature.

Table 4 Effect of Temperature on Epoxidation of methyl oleate. [12]

entry	T (°C)	C (%)	monoepoxide (%)	diepoxide (%)	total epoxides (%)
1	5	77.8	28.7	49.3	63.7
2	15	84.3	15.1	59.2	66.8
3	25	100.0	4.7	90.4	92.8
4	35	100.0	2.5	87.9	89.2
5	45	100.0	0.0	82.1	82.1

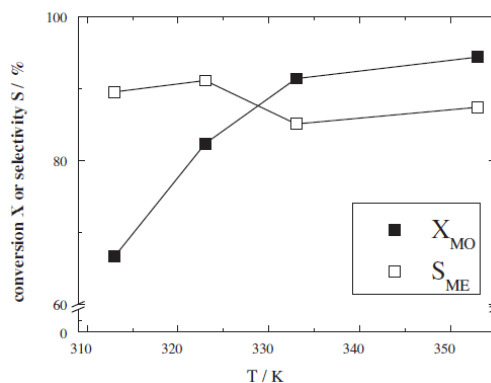


Figure 5 Effect of reaction temperature on conversion of methyl oleate X_{MO} and epoxide selectivity S_{ME} in the epoxidation of methyl oleate over TS-1. [2]

2.1.4. Effect of solvent

The solubility of FAMES and oils in hydrogen peroxide solution is limited. To obtain a homogenous of hydrogen peroxide and methyl ester solvent is required. According to **Table 5.** and Turco et al. (2016) [13], Solvent has affected to both conversion and selectivity. However, different substrates are suitable with different solvents. Polarity and the protic/aprotic nature of solvent are also affected on conversion and selectivity of epoxidation.

Soybean oil showed good activity with ethyl acetate. Due to the production of acetic acid in the final product, this acetic acid can react with hydrogen peroxide and convert to peracetic acid. Peracetic acid can promote the higher conversion of epoxidation. However, the presence of peracetic acid promotes the degradation of epoxide by ring opening reaction. On the other hand, soybean oil showed low activity with acetonitrile. This can be explained that oil is poorly dissolved in acetonitrile. Acetonitrile fills most of pore volume of catalyst, so soybean oil can not react with the active sites.

By the way, acetonitrile is suitable for methyl ester such as methyl oleate. Due to, the high polarity of acetonitrile ($\epsilon = 37$). This can be explained by considering to the solubility of both reactants and solvent. Methyl oleate is miscible in all solvent, hydrogen

peroxide and water are soluble in high polarity solvent. The physical properties of acetonitrile and hydrogen peroxide were list in Table 6 and Table 7.

Table 5 Influence of the solvent on the initial rate of reaction, conversion of methyl oleate X_{MO} , selectivity S_{ME} and conversion of hydrogen peroxide $X_{H_2O_2}$ in the epoxidation of methyl oleate over TS-1 (Ind.) at 323 K after 24 h. [2]

Solvent	Initial Rate r_0 (mol l ⁻¹ h ⁻¹)	Conversion X_{MO} (%)	Selectivity S_{ME} (%)	Conversion $X_{H_2O_2}$ (%)
Ethylacetate	0.025	98	36	72
Acetone	0.024	92	52	36
Acetonitrile	0.021	93	87	97
Acetonitrile/ methanol	0.016	79	85	62
Diglyme	0.015	79	84	66
Methanol	0.002	20	17	57
Diisopropylether	0.005	4	31	67

Table 6 Physical properties of acetonitrile.

Properties	Information
Molecular weight	41.05 g/mol
Density	0.786 g/ml at 25 °C
Melting point	-48 °C (lit)
Normal boiling point	81 - 82 °C (lit)
Vapor pressure	72.8 mmHg (20 °C)

Table 7 Physical properties of hydrogen peroxide.

Properties	Information
Molecular weight	34.01 g/mol
Density	1.11 g/ml

2.1.5 Effect of reaction time

Both conversions of methyl oleate and selectivity of methyl oleate epoxide show as a function of reaction time. According to **Figure 6**, the rate of epoxidation reaction was increased with reaction time. However, both the rate of epoxidation reaction of methyl oleate and degradation of hydrogen peroxide strongly rose at first 5 h of the reaction. The degradation of hydrogen peroxide converts hydrogen peroxide to H^+ and H_2O . Since the degradation of hydrogen peroxide occurred with increasing reaction time. In agreement with **Figure 4**, the side reaction of epoxidation was existing. Then, the selectivity of methyl oleate epoxide was decreased with increasing reaction time. [2, 6] After 5 h of reaction time the conversion of epoxidation was slightly slow down. Since Ti leaching or adsorbed reaction residues hindering the access of the active site.

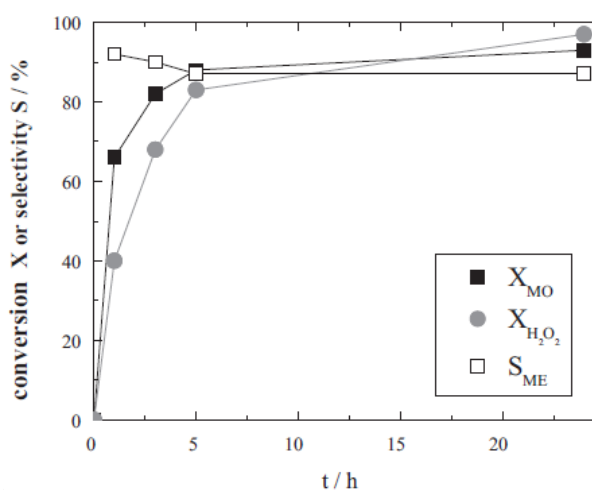


Figure 6 Conversion and selectivity as a function of time of methyl oleate epoxide. [2]

2.2. TiO_2

Titanium dioxide (TiO_2) which is also known as titania, has been widely used as a pigment in paints, catalysts, catalysts supported, filter coating cosmetics and foodstuffs. Therefore, it is claimed that titanium dioxide is one of the common materials due to its non-toxicity, low cost, and relatively high chemical stability [27, 28]. Titanium dioxide exists in both crystalline and amorphous forms. However, titanium dioxide has three major crystalline phases. First is rutile, the most stable phases with small crystals size below 11 nm. Second is anatase, with large crystals size above 35 nm. Third is brookite,

with crystals size between anatase and rutile. According to **Figure 7**, those three phases indicate different TiO_2 crystal structures. Rutile and anatase are reported more than brookite, due to their higher activity. The most active phase is anatase phase. The most stable phase at high temperature is rutile. Rutile can be observed at temperature between 400 to 800 °C [29-31]. The physical properties of TiO_2 and their three different phases were listed in **Table 8**. According to **Table 8**. Anatase has crystal system as tetragonal with dipyramidal habit, which is mainly used in photocatalyst under UV irradiation. However, rutile also has a tetragonal crystal structure with prismatic habit. Therefore, rutile is mostly used as pigment in paint [31, 32].

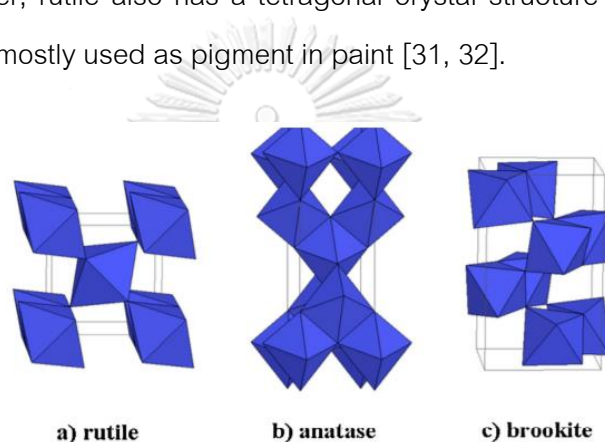


Figure 7 TiO_2 crystal structures: rutile (a), anatase (b) and brookite (c). Ti^{4+} sits at the center of the octahedron and O_2 at each corner. [31]

Table 8 Physical properties of TiO_2 .

Properties	Information
Molecular weight	79.866 g/mol
Melting point	1844 °C
Normal boiling point	2973 °C
Crystal system	
Anatase	Tetragonal
Rutile	Tetragonal
Brookite	Orthorhombic
Density	
Anatase	3830 kg/m ³

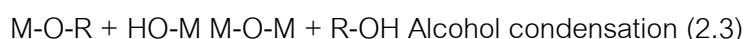
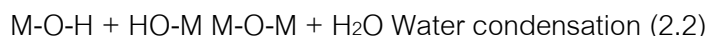
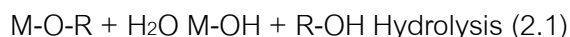
Properties	Information
Rutile	4240 kg/m ³
Brookite	4170 kg/m ³

Titanium dioxide is mostly used as semiconducting transition metal oxide. Moreover, TiO₂ are used in solar cells, photocatalytic, chemical sensor, self-cleaning, environmental purification, pigments, adsorbents, paints, paper, plastic, cosmetics, catalytic and medical [33]. TiO₂ can be synthesis be many methods such as sol-gel, microemulsion, flame synthesis, ultrasonic irradiation, oxidation hydrothermal synthesis, and hydrolysis precipitation. However, the different synthesis methods give different properties of TiO₂. Moreover, the same synthesis methods using different starting materials, amounts of materials, solvent or temperature result in different TiO₂ properties [34-37].

Sol-gel method is the best method to synthesize ultra-fine metallic oxide and nanocrystalline TiO₂. The sol-gel method formation follows by **Scheme1**. Moreover, the physical properties of TiO₂ can be easily modified by using sol-gel method. This method is carried out in solution and prepared in mild condition (low temperature and pressure). A typical example of the former approach is dispersion of oxides or hydroxides in water with the pH adjusted so that the solid particles remain in suspension rather than precipitate out. A typical example of the later approach is the addition of metal alkoxide to water. The alkoxide is hydrolyzed giving the oxide as a colloidal product. This method gives nanometer-sized of TiO₂ with high purity. However, sol-gel method derived amorphous products. Therefore, heat treatment at high temperature to obtain crystalline products. Calcination process results in reduction of surface area and phase transformation. Sol-gel process is the evolution of inorganic networks through the formation of sol (colloidal suspension) and gelation of sol to form a network in the gel (continuous liquid phase).[38] A sol is a dispersion of solid powder in liquid suspension solution. Sol is formed from hydrolysis and polymerization reaction of precursors, which usually use inorganic metal salts or metal organic compounds. However, metal

alkoxides are mostly used because its react with water. Complete polymerization and loss of solvent lead to transformation of liquid sol to solid gel phase. A gel has both liquid and solid state, which presents a solid network filled in liquid components.[34, 39]

Scheme. 1 The formation of sol-gel process.



2.3. TiO_2/SiO_2

Silica supported of metal oxides catalysts present of a higher percentage of metal oxide dispersion. TiO_2/SiO_2 catalysts have higher mechanical strength, thermal stability and surface area than pure TiO_2 . Silica surface has hydroxyls group. Due to their hydrophilic character, it can be both adsorptive or reactive sites. The different types of titanium species present a distinguish kinds of TiO_x species (tetrahedral and octahedral coordination). Hydrophobicity catalyst decreases the side reaction of epoxidation. According to **Figure 8**, water played an important role in epoxidation reaction. When water adsorbs on Ti active site, titanium change coordination from tetrahedral to octahedral. Whereas, hydrogen peroxide leads to the formation of $Ti-OOH$ (an activated intermediate) [14]. According to **Figure 9** and **Figure 10**, show the surface hydroxyl group of TiO_2/SiO_2 . Which different silica support give different surface hydroxyl group. Due to the different structure of silica support.

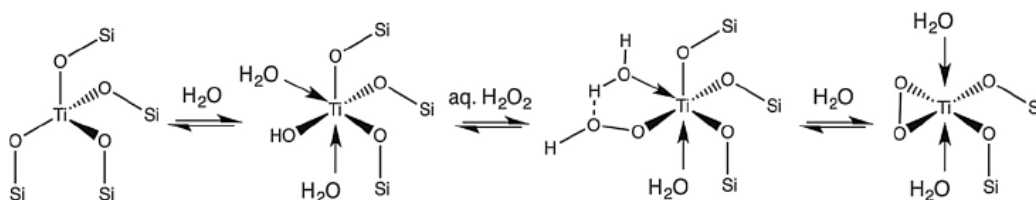


Figure 8 Mechanism of inactivation of amorphous titanasilicate epoxidation catalysts in presence of water.[14]

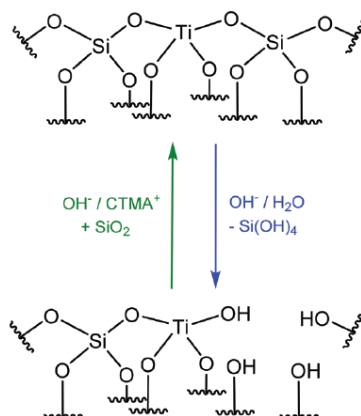


Figure 9 Surface hydroxyl group of TiO₂/Silicalite.[8]

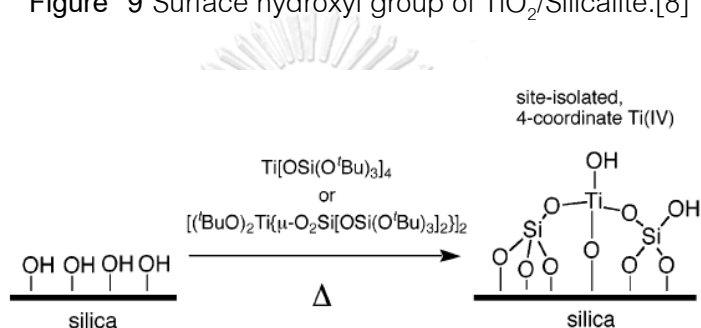
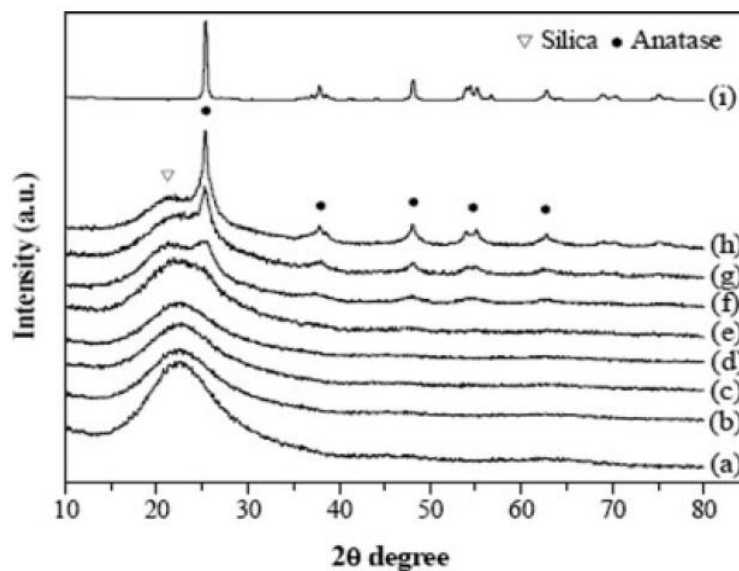


Figure 10 Surface hydroxyl group of TiO₂/SBA-15. [40]

TiO₂/SiO₂ catalysts have been widely study such as varies of Ti loading and calcination temperature. As shown in Figure 11 and Figure 12 TiO₂/SiO₂ was used in transesterification reaction, the more Ti loading and calcination temperature gave more TiO₂ peak in anatase form. According to Table 9 and Table 10, conversion and selectivity decreased when the TiO₂ peaks occurred. TiO₂ peaks were detected at 14% Ti loading and calcination temperature at 600^oC. Therefore, Ti loading more than 14% and calcination temperature more than 600^oC gave less in both conversion and selectivity of transesterification. Both conversion and selectivity decrease when increasing Ti% loading and calcination temperature because of TiO₂ block pore mouth of catalysts. [20]

The most important peak from FTIR was 960 cm⁻¹, which show Ti-O-Si. According to Figure 13 and Figure 14, more Ti loading give more absorbance of Ti-O-Si. The active site of epoxidation reaction is TiO₂ in tetrahedral coordination form, which can detect by both UV-vis and XPS. According to Figure 15, Ti in tetrahedral coordinate was

detected 465.4 eV for Ti^{4+} $2p_{1/2}$ and 458.8 eV for Ti^{4+} $2p_{3/2}$. The peaks shift to lower eV due to Ti^{3+} was detected. As shown in Figure 16, the UV-vis spectra of Ti^{4+} was detected



at 215 nm. However, 295 nm was occurred due to Ti with 5 or 6 coordination. [41-43]
 Figure 11 XRD patterns of TiO_2/SiO_2 catalysts with different TiO_2 loadings: (a) support; (b) 1%; (c) 5%; (d) 10%; (e) 12%; (f) 14%; (g) 16%; (h) 20%; and (i) nano anatase TiO_2 . [20]

TiO_2 Loadings (wt %)	Conversion* (%)	Selectivity (%)			Yield (%)	
		AN	MPO	DPO	MPO	DPO
1	42.9	0.6	80.8	18.3	34.3	7.9
5	51.5	0.6	76.7	22.7	39.5	11.7
10	62.3	0.7	74.2	25.0	46.2	15.6
12	66.3	0.6	73.9	25.3	49.0	16.8
14	65.9	0.7	74.1	25.1	48.8	16.5
16	62.4	0.8	75.2	23.4	46.9	14.6
18	56.8	0.9	76.4	22.5	43.4	12.9
20	50.8	1.0	77.4	21.4	39.3	10.9

Reaction conditions: 0.1 mol DMO, 0.3 mol phenol, 1.8 g catalyst (calcined at 550 °C), conducted at 180 °C for 2 h.

*Based on charged DMO.

Table 9 Catalytic Activity of TiO_2/SiO_2 catalysts with Different TiO_2 Loadings. [20]

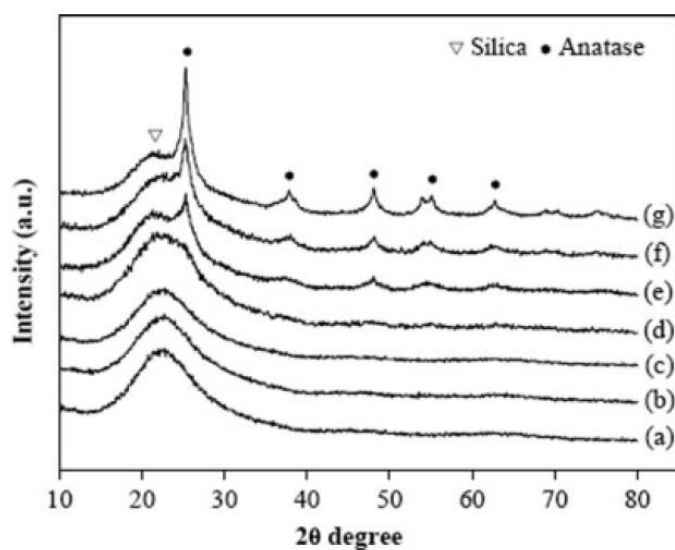


Figure 12 XRD spectra of 12 wt% $\text{TiO}_2/\text{SiO}_2$ catalysts under different calcination temperature: (a) 300°C ; (b) 400°C ; (c) 500°C ; (d) 550°C ; (e) 600°C ; (f) 700°C ; and (g) 800°C . [20]

Calcination Temperature ($^\circ\text{C}$)	Conversion* (%)	Selectivity (%)			Yield (%)	
		AN	MPO	DPO	MPO	DPO
300	48.8	2.1	78.3	19.1	38.2	9.3
400	49.2	1.0	79.1	19.7	38.9	9.7
500	58.1	0.7	74.2	25.0	43.1	14.5
550	66.3	0.6	73.9	25.3	49.0	16.8
600	65.4	1.1	74.6	24.0	48.8	15.7
700	62.1	1.2	76.7	21.6	47.6	13.4
800	52.6	1.5	81.7	16.3	43.0	8.6

Reaction conditions: 0.1 mol DMO, 0.3 mol phenol, 1.8 g catalyst (12 wt% TiO_2 loading), conducted at 180°C for 2 h.

*Based on charged DMO.

Table 10 Effect of Calcination Temperature on Catalytic Properties of $\text{TiO}_2/\text{SiO}_2$. [20]

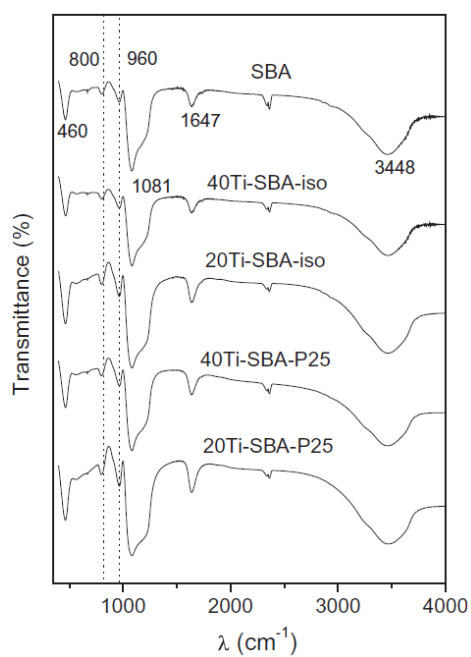


Figure 13 FTIR spectra of samples. [42]

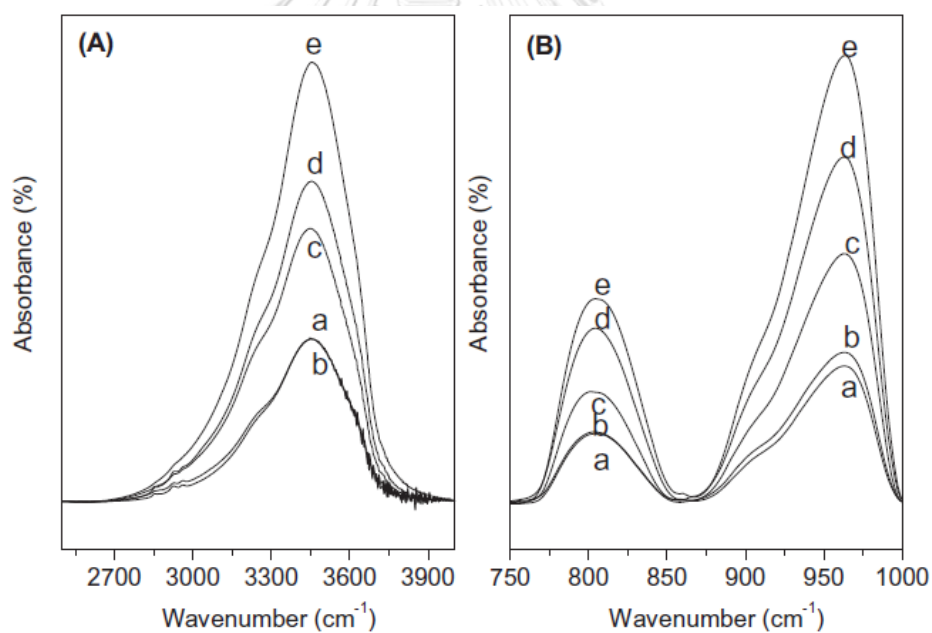


Figure 14 FTIR region in absorbance mode: (a) SBA-15; (b) 40Ti-SBA-iso; (c) 20Ti-SBA-iso; (d) 40Ti-SBA-P25 and (e) 20Ti-SBAP25. [42]

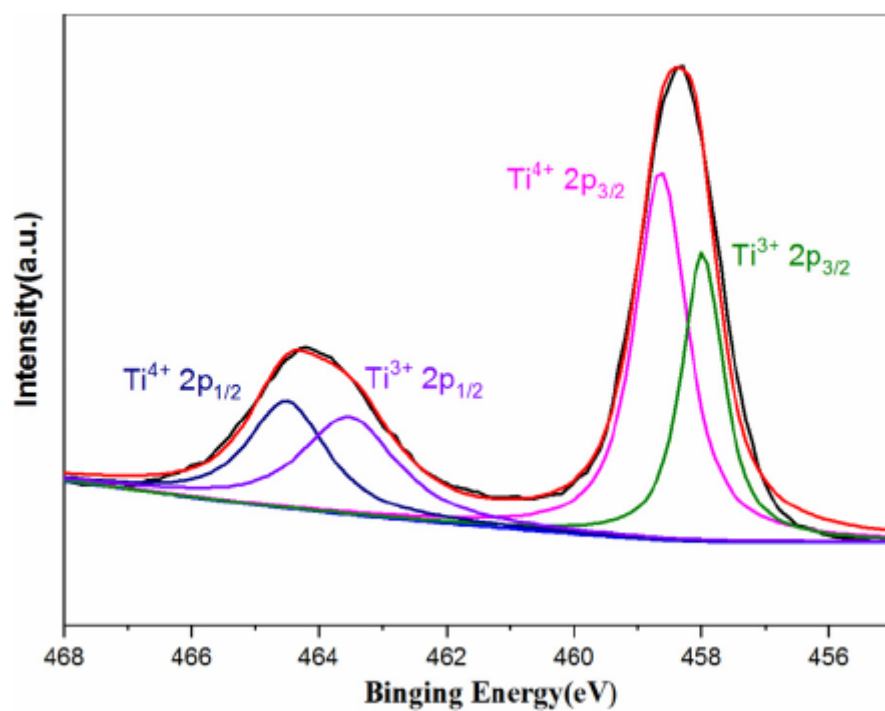


Figure 15 XPS spectra of Ag-Ti nanotubes after self-doped Ti³⁺. [43]

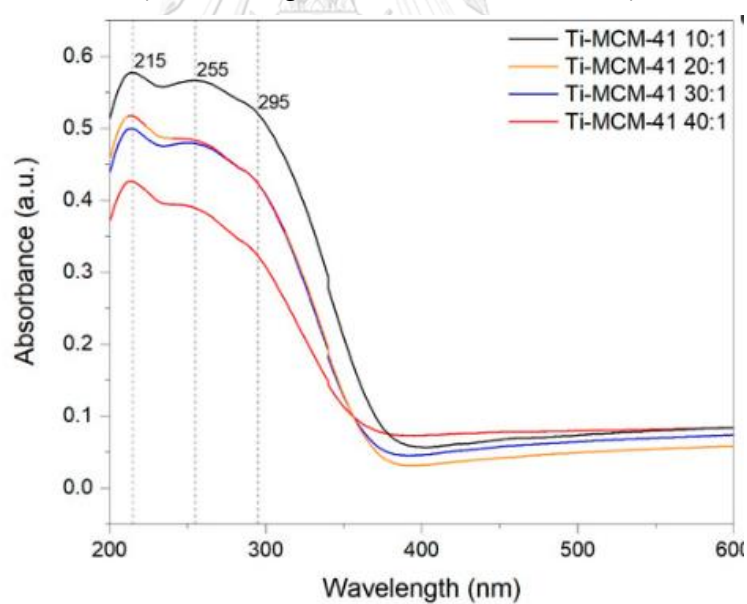


Figure 16 UV/vis spectra of the Ti-MCM-41 catalysts with different molar ratios of Si:Ti in the crystallization gel (respectively, 40:1, 30:1, 20:1, and 10:1). [41]

2.4. Other catalyst for epoxidation reaction

The commonly catalysts for epoxidation reaction of methyl oleate are $\text{TiO}_2/\text{SiO}_2$, TS-1 and Ti-MCM-41. However, there are many kinds of metal oxide catalyst in epoxidation reaction. Examples of other catalysts are shown in Table 11.

Table 11 Other catalysts for epoxidation reaction.

catalyst	oxidant	T (°C)	solvent	Ref
2- percarboxyethy lfunctionalized silica	Oxidant add in catalyst	25	dichloromethane	[12]
TiMCM-41	tert- butylhydroperoxide	90	ethyl acetate	[6]
Ti/SiO ₂	hydroperoxide	50	acetonitrile	[2]
TS-1				
Ti-MCM-41				
TiO _x -SiO ₂				
WO _x -Al ₂ O ₃				
MoO _x -Al ₂ O ₃				
MoO _x -SiO ₂				
TS-1	hydroperoxide	50	acetonitrile	[8]
manganese(IV) complex [LMn(O) ₃ MnL](PF ₆) ₂	Hydroperoxide	25	acetonitrile	[44]
MoO _x encapsulated inside hollow silica spheres	tert-Butyl hydroperoxide	80	1,2- Dichloroethane	[45]

catalyst	oxidant	T (°C)	solvent	Ref
peroxophospho tungstate	hydrogen peroxide	35-40	-	[18]
MoO ₃ /Bipyridin edicarboxylate Hybrid	tert-Butyl hydroperoxide	55, 75	benzene	[19]
H ₅ PV ₂ Mo ₁₀ O ₄₀	sodium sulfite oxygen	65	Acetic acid	[46]
Nb/Al ₂ O ₃	hydrogen peroxide	80	acetonitrile	[47]
Nb/SiO ₂				
Polyoxometalat e-Paired Polymer Coated Fe ₃ O ₄	hydrogen peroxide	70,75	acetonitrile	[17]
Al ₂ O ₃	hydrogen peroxide	80	acetonitrile	[13]

CHAPTER III

EXPERIMENTAL

In this chapter, it consists of the detail of chemicals, catalyst preparation, characterization and catalytic epoxidation reaction of methyl oleate test.

3.1. Materials and chemicals

The chemicals used in both catalyst preparation and epoxidation are listed in Table 12 and Table 13, respectively.

Table 12 Chemicals used in catalyst preparation.

Chemicals	Chemicals name	Purity (%)	Suppliers
$\text{TiOCH}(\text{CH}_3)_{24}$	Titanium (IV) isopropoxide	97	Aldrich
HNO_3	Nitric acid	70	Asia pacific specialty chemical limited
$\text{C}_2\text{H}_5\text{OH}$	Ethanol absolute	100	Merck
SiO_2	Silica, fumed	99.8	Aldrich
SiO_2	Silica gel	99.8	Sigma-Aldrich
$\text{C}_6\text{H}_{12}\text{O}$	cyclohexanol	99	Aldrich

Table 13 Chemicals used in epoxidation reaction.

Chemicals	Chemicals name	Purity (%)	Suppliers
$\text{C}_{19}\text{H}_{36}\text{O}_2$	Methyl oleate	99	Aldrich
H_2O_2	Hydrogen peroxide	30 (w/w) in H_2O	Aldrich
C_{10}H_8	naphthalene	>98	Fluka
CH_3CN	acetonitrile	99.8	Aldrich

3.2. Preparation of catalyst

3.2.1 Synthesis of TiO_2 by sol-gel method

A sol-gel method was used to prepare titanium dioxide by using titanium isopropoxide as a precursor. The method began with 7.33 ml of 70% nitric acid was added to 1,000 ml of deionized water as the acid solution was stirring. Then 83.33 ml of titanium isopropoxide was poured slowly and the suspension appeared. The suspension was stirred continuously around 3 days or until sol became clear. In this step sol has pH around 1. Therefore titanium dioxide sol was dialyzed in a cellulose membrane with a molecular weight cutoff of 3500 (Spectrum companies, Gardena, CA) by deionized water until pH of sol became 3.5. The dialyzed sol was dried at 110°C overnight, crushed, ground and the calcined at 100°C , 200°C , 300°C , 400°C and 500°C for 2 hours with a heating rate $10^\circ\text{C}/\text{min}$.

3.2.2 Synthesis of TiO_2 with SiO_2 supported by incipient wetness impregnation method

Silica supported are fumed silica, silicalite, SBA-15, MCM-41 and silica gel. First, 5 g. of silica supported was heated at 110°C overnight. Then titanium isopropoxide 0.52 mL was added in absolute ethanol. The volume of ethanol base on pore volume of the silica supported. The titanium isopropoxide solution was dropped to silica supported at room temperature until it became slurry. The catalyst product was dried at room temperature for 1 h. Then dried at 110°C overnight. The solid catalyst crushed into fine powder, following by calcination at 550 K under air for 5 h to get white powder of $\text{TiO}_2/\text{SiO}_2$.

3.2.3 synthesis of TiO_2 /fumed SiO_2 by incipient wetness impregnation method

5 g of fumed-silica was dried at 110°C overnight. Then titanium isopropoxide 0.3 mmol (0.89 mL) was added in absolute ethanol. The volume of ethanol was 2.3 mL (base on pore volume of the fumed silica supported which 0.64 mL/g). The titanium isopropoxide solution was dropped to silica supported at room temperature until it

became slurry. The catalyst product was dried at room temperature for 1 h. Then dried at 110°C overnight. The solid catalyst crushed into fine powder, following by calcination at 550 K under air for 5 h to get white powder of TiO₂/SiO₂.

3.2.4 Synthesis of TiO₂/fumed SiO₂ by wet impregnation method

Fumed silica was dried overnight (at 110 °C). Titanium isopropoxide solution was prepared by 0.3 mmol (0.89 cm³) of titanium isopropoxide and 5 mL absolute ethanol. 5 g. of fumed-silica was added and stirred with titanium isopropoxide solution at 50 °C for 5 h. Then dried at 110 °C overnight. The solid was crushed into fine powder, followed by calcination at 550 °C under air for 5 h to obtain TiO₂/SiO₂.

3.2.5 Synthesis of TiO₂/fumed SiO₂ by grafting method

5 g of fumed-silica was dried at 110°C overnight. Then 0.3 mmol (0.89 cm³) of titanium isopropoxide was added in cyclohexanol. Fumed-silica was added to titanium isopropoxide solution (C_{TIP} = 0.02 mol/l) under reflux at 160 °C for 2 h. Then dried at 110 °C overnight. Then crushed and calcined at 550 °C under air for 5 h to obtain white powder of TiO₂/SiO₂. [2]

3.2.6 Synthesis of TiO₂/ fumed SiO₂ with different Ti loading by incipient wetness impregnation method

First, 5 g. of fumed silica was dried at 110°C overnight. Then titanium isopropoxide 0.52, 0.89, 1.26 and 1.63 cm³ added in 3, 2.48, 2.21, 1.84 and 1.47 cm³ absolute ethanol respectively. The titanium isopropoxide solution was dropped to fumed silica supported at room temperature until it became slurry. The catalyst product was dried at room temperature for 1 h. Then dried at 110°C overnight. The solid catalyst crushed into fine powder, following by calcination at 550 °C under air for 5 h to get white powder of TiO₂/SiO₂.

3.3. Catalyst characterization techniques

3.3.1. N₂-physisorption

The surface area, pore volume and pore diameter were measured by the Brunauer–Emmet–Teller (BET) method on a Micromeritics ASAP 2020 instrument. The measurements were performed with nitrogen as adsorbate at liquid nitrogen temperature following the samples pretreatment at 200 °C under vacuum 12 h. Sample of N₂-physisorption was heated at 110 °C overnight before analyzing.

N₂ physisorption was carried out on a micromeritics chemisorb 2750 to determine the specific area at the single point of TiO₂/SiO₂ by using 30% N₂/He after preheat sample at 200 °C for 1 h.

3.3.2. Scanning electron microscope (SEM) and energy dispersive X-ray spectroscopy (EDX)

The morphologies of catalysts were determined by scanning electron microscope (SEM) which operated by using a model of JEOL mode JSM-6400. The elemental distribution on a surface were investigated by energy dispersive X-ray spectroscopy (EDX) that was performed by using Link Isis series 300 program. Sample of SEM-EDX was heated at 110 °C overnight before analyzing.

3.3.3. X-ray Diffraction (XRD)

The X-ray diffraction (XRD) patterns were analyzed by X-ray diffractometer (Bruker D8 Advance) using Cu K α irradiation at range between 20 ° to 80 ° with a scan speed 0.5 sec/step for TiO₂. X-ray diffractometer (Bruker D8 Advance) using Cu K α irradiation at range between 1.2 ° to 50 ° with a scan speed 0.5 sec/step for TiO₂/SiO₂. The lattice parameter and d-spacing were calculated based on Bragg's law. Crystallite size was calculated by Scherrer equation.

3.3.4. UV-visible spectroscopic analysis (UV-vis)

UV-vis analysis was used to obtain the information about the coordination geometry of Ti cations and the ligand environment. The absorption range is 200 to 500 nm obtained by Perkin Elmer Lambda 650 spectrophotometer. The step size for the scan was 1 nm.

3.3.5 Fourier transform infrared spectroscopy (FT-IR)

FT-IR analysis was used to provide functional group as a chemical structure of the catalyst. FT-IR was obtained by using a Nicolet 6700 FT-IR spectrometer. Catalyst was performed on compacted powder disk of 0.5-1 g of each catalyst.

3.3.6 X-ray photoelectron spectroscopy (XPS)

The binding energy of each core atomic orbital of catalysts was determined by AMICUS spectrometer which using MgK α X-ray radiation (1253.6 eV) and AlK α X-ray radiation (1486.6 eV) at voltage 15kV and current of 12 mA. The pressure in the analysis chamber was less than 10⁻⁵ Pa. The small amount of sample was brought to pretreat at 110°C for 24 hours before the analysis.

3.3.7 Thermogravimetric analysis (TGA)

The amount of carbon content in the catalyst was determined by TA Instruments SDT Q 600 analyzer, which measures the amount of weight changed of material after reaction testing and provided the chemical phenomena such as decomposition temperature (finding reaction temperature range), and solid-gas reactions (oxidation). The samples of 10-20 mg and a temperature ramping from 298 to 1273 K at 2 K/min were used in the operation with N₂ UHP carrier gas.

3.4 Catalytic activity on epoxidation reaction

3.4.1. Epoxidation reaction

The preparation of the substrate solution is listed in **Table 14**. First, drop naphthalene in acetonitrile. Then add methyl oleate to this solution.

Table 14 list of substrate solution.

Chemicals	Volume (ml)
C ₁₉ H ₃₆ O ₂ (MO)	0.1
C ₁₀ H ₈	10
CH ₃ CN	0.06

Catalytic epoxidation tests were carried in a 50 cm³ three necked round-bottom glass reactor with a reflux condenser. The reactor was heated in an oil bath with constant reaction temperature at 50^oC and magnetic stirring at 500 rpm. First, add 300 mg of catalyst in the reactor. Follow by addition of substrate solution and wait until substrate solution became 50^oC. Then add 70 mg of hydrogen peroxide. The epoxidation starts at the time hydrogen peroxide was added. Samples 0.2 mL were taken from the reaction mixture after 1, 2, 3, 4 and 5 h of reaction. The catalyst was removed from the samples by filtration. The sample was analyzed by gas chromatography.

$$\text{Conversion \%} = \frac{\text{Moles of methyl oleate (in)} - \text{Moles of methyl oleate (out)}}{\text{Moles of methyl oleate (in)}} \times 100$$

$$\text{Selectivity \%} = \frac{\text{Moles of methyl oleate epoxide}}{\text{Moles of methyl oleate (in)} - \text{Moles of methyl oleate (out)}} \times 100$$

3.4.2. Reaction products analyzed

The reaction mixtures were analyzed by gas chromatography-mass spectroscopy (GC-MS) and gas chromatography with flame ionization detector (GC-FID). GC-MS instruments were equipped with a DB-5 column (30 m x 0.25 mm x 0.25 um). GC-FID instruments were equipped with a Rtx-5 column (30 m x 0.32 mm). According to **Table 15**, the temperature of column increased from 180^oC to 250^oC then hold 10 min, at heating rate 5^oC/min. Temperature of injector and detector was 250^oC.

Table 15 list of gas chromatography condition.

Gas chromatograph	Shimadzu GC2014	Shimadzu GC2014
Detector	FID	FID-MS
Capillary column	Rtx-5	DB-5
Carrier gas	Helium (99.99 vol.%)	Helium (99.99 vol.%)
Make-up gas	Air (99.9 vol.%)	Helium (99.99 vol.%)
Column temperature	180 °C	180 °C
Injector temperature	250 °C	250 °C
Detector temperature	250 °C	250 °C

CHAPTER IV

RESULTS AND DISCUSSION

The results and discussion in this chapter consist of four parts, including the effect of calcination temperature (100, 200, 300, 400 and 500 °C) of TiO₂ by sol-gel method, the second part, the effect of SiO₂ support (fumed silica, silica gel, silicalite, MCM-41 and SBA-15) of TiO₂/SiO₂ by incipient wetness impregnation method, the third part, the effect of TiO₂/fumed SiO₂ synthesis method (incipient wetness impregnation method, wet impregnation method and grafting method), and the fourth part, the effect of Ti loading (7,12,17,22 and 27% TIP) of TiO₂/fumed SiO₂ by incipient wetness impregnation method. The catalyst characteristics were investigated by SEM-EDX, XRD, FTIR, UV-vis, XPS, N₂ physisorption and TGA.

4.1. Epoxidation of TiO₂ catalysts with different calcination temperatures

4.1.1. Catalytic activity and selectivity of TiO₂ catalyst

Catalytic activity of TiO₂ catalysts for epoxidation of methyl oleate is shown in **Figure 17**. The highest catalytic activity of commercial TiO₂ is commercial TiO₂ type B with 38.86% conversion. Moreover, the lowest catalytic activity of commercial TiO₂ is the commercial TiO₂ type A with 11.32% conversion. For TiO₂ by sol-gel method, 100°C and 200°C calcination temperature have same catalytic activity around 40% conversion. Moreover, 300°C calcination temperature have highest catalytic activity around 75% conversion. However, 400°C and 500°C calcination temperature has lower catalytic activity than 300°C but higher than 100°C and 200°C, which catalytic activity around 65% conversion. According to **Figure 18**, selectivity of epoxidation showed the same trend as the catalyst activity that 300°C calcination temperature gave highest selectivity of epoxidation of methyl oleate. However, 100°C and 200°C TiO₂ showed lower selectivity of epoxidation. Since 100°C and 200°C are complex TiO₂.

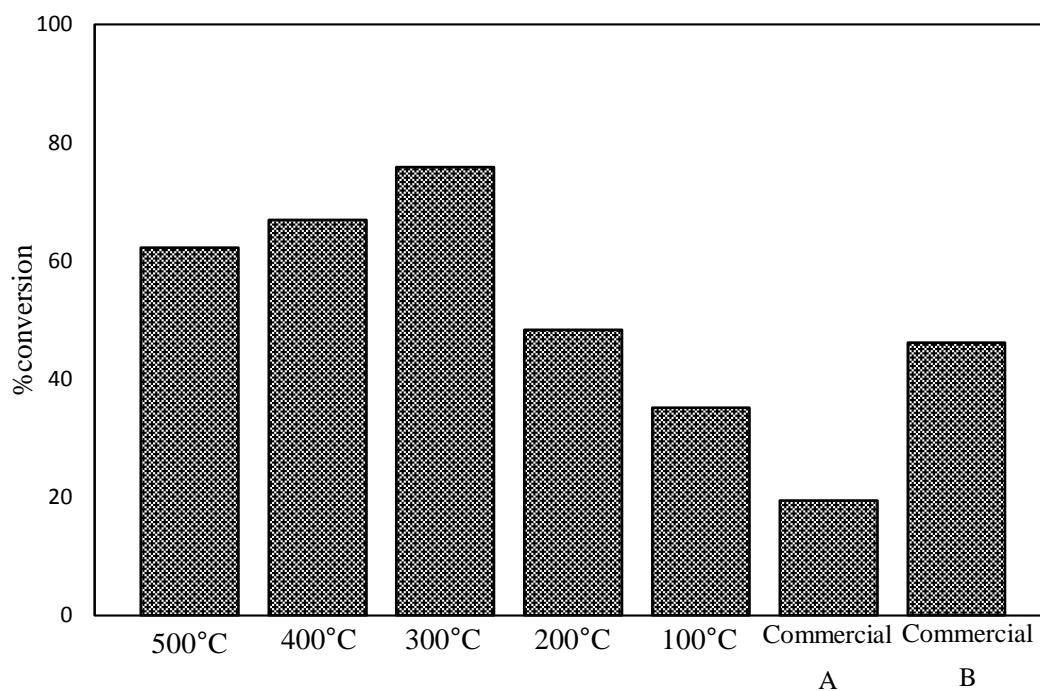


Figure 17 Conversion of all TiO_2 catalysts in epoxidation of methyl oleate at 5 h.

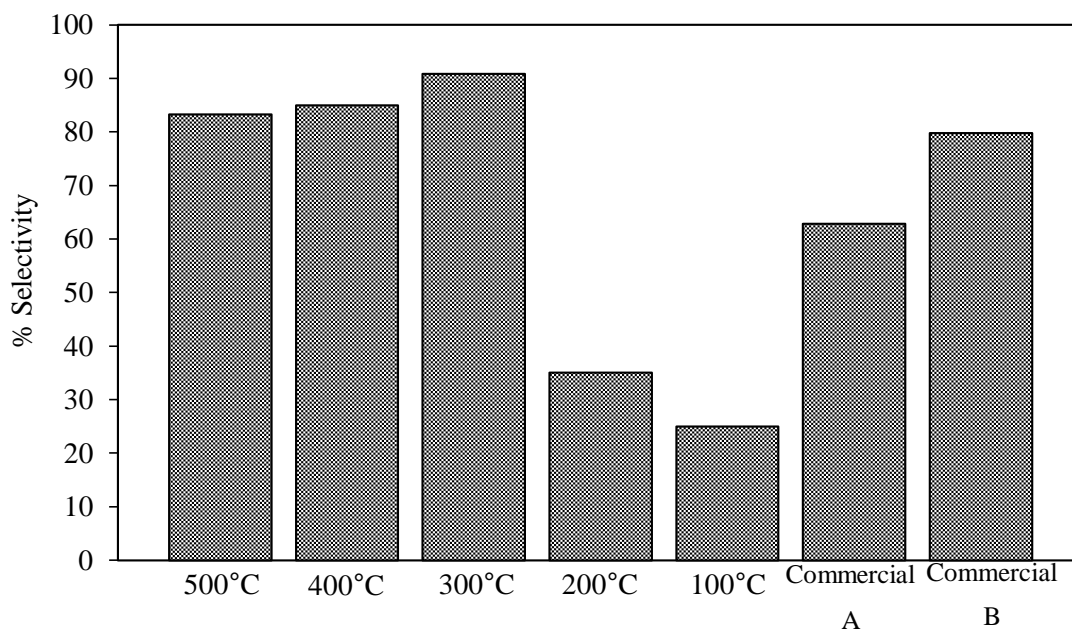


Figure 18 Selectivity of all TiO_2 catalyst in epoxidation of methyl oleate at 5 h.

4.1.2. Characterization of TiO₂ catalyst

According to **Table 16**, 500°C TiO₂ has lower anatase weight fraction and surface area than both 300°C and 400°C TiO₂. Moreover, 500°C has highest crystallinity of TiO₂ catalyst by sol-gel method. The crystal sizes of TiO₂ were calculated from the half-width of peaks using Scherrer's equation ($d = 0.9\lambda/\beta\cos\theta$). The size of the anatase phase was calculated from $2\theta = 25.3^\circ$. The weight fraction of the anatase phase was calculated from $2\theta = 25.3^\circ$ and 48.1. Calcination temperature above 300°C, the anatase crystal size was a function of calcination temperature. The increasing of calcination temperature resulted in a slightly increase of the anatase crystal size from 5.0 nm at temperature 100 °C to 9.9 nm at 500°C. Both commercial TiO₂ showed higher anatase crystal size than TiO₂ catalysts from sol-gel method. Commercial TiO₂ type A showed the highest anatase crystal size at 18.3 nm. However, commercial TiO₂ type B exhibited the anatase crystal size at 11.3 nm. The anatase weight fraction was higher at low temperature and slightly decrease at high temperature. Calcination temperature at 100 °C anatase weight fraction exhibited of 90.6 wt.% . However, at 500 °C calcination temperature the anatase weight fraction decrease to 56.2 wt.% . The highest anatase weight fraction was commercial TiO₂ type B, which show 99.7 wt.% of anatase. On the other hand, commercial TiO₂ type A showed 86.5 wt.% of anatase, which higher than calcination temperature 300 °C, 400 °C and 500 °C. However, TiO₂ catalyst by sol-gel method found that higher calcination temperature gave higher crystallinity. The highest crystallinity of all TiO₂ catalyst was commercial TiO₂ type A, which exhibit 41.9% crystalline. the lowest was commercial TiO₂ type B, which showed 10.2% crystalline. Anatase crystallite size of TiO₂ grew with increasing calcination temperature. On the other hand, the specific surface area of TiO₂ decreased from 188 m²/g to 73 m²/g. The sintering at surface of TiO₂ is affected from high temperature. However, the more surface area, the more catalyst activity occurs because larger surface area implies higher number of active site[34].

XRD pattern of TiO₂ catalysts calcined at various temperatures and commercial TiO₂ were characterized by the bulk crystalline structures of TiO₂ the results are shown in Figure 19. When the calcination temperature below 400 °C, anatase was the domain phase, with peaks at $2\theta = 25.3^\circ, 37.8^\circ, 48.1^\circ, 54.0^\circ$ and 55.1° . TiO₂ from sol-gel method was also found small brookite phase peak at $2\theta = 30.8^\circ$. Rutile phase appeared above 300 °C and normally become domain at 600 °C [29, 34, 38]. Moreover, crystallinity at high temperature was higher than the low temperature. XRD pattern of commercial TiO₂ type A showed both anatase and rutile phase without brookite phase. However, commercial TiO₂ type B showed anatase as the main phase. In addition, commercial TiO₂ type A showed a sharper peak than commercial TiO₂ type B.

Table 16 Crystallite size, Anatase weight fraction and %crystalline of TiO₂ catalysts.

Catalyst	Crystallite size (nm)	Anatase weight fraction (wt.%)	%crystallinity	Surface area (m ² /g)
Commercial A	18.3	86.5	41.9	35
Commercial B	11.3	99.7	10.2	112
500°C	9.9	56.2	24.9	73
400°C	7.5	77.5	21.1	111
300°C	7.2	80.7	18.5	147
200°C	5.0	90.4	15.4	174
100°C	4.9	90.6	14.5	188

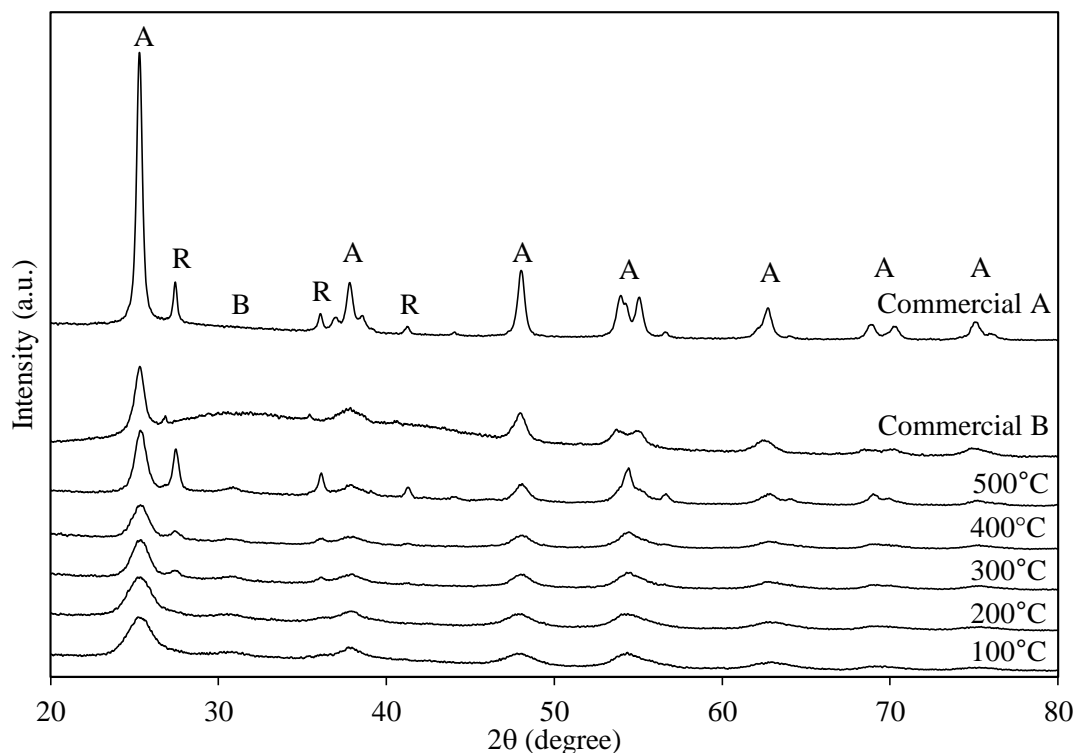


Figure 19 X-ray diffraction pattern of all TiO_2 catalysts prepared by sol-gel method and commercial TiO_2 .

Figure 20. shows the FT-IR spectra of all TiO_2 sol-gel catalysts. The spectrum of TiO_2 calcined at 100°C has several characteristic absorptions peak: Peak observed at $3200 - 3100 \text{ cm}^{-1}$ correspond to stretching vibration of O-H bond. Peak observed at 2162 cm^{-1} correspond to the weak band $\text{C} \equiv \text{C}$ stretching vibration. The little peaks at 2020 cm^{-1} and 1975 cm^{-1} correspond to $\text{C}=\text{C}=\text{C}$ Stretching. Peaks at 1738 cm^{-1} and 1637 cm^{-1} correspond to stretching vibration of $\text{C}=\text{O}$ bond. In addition, peak at 1637 cm^{-1} corresponds to stretching vibration of $\text{H}-\text{O}-\text{CH}_2$ and $\text{H}-\text{O}-\text{H}$ bending of absorbed water. Peaks observed at 1365 cm^{-1} and 1215 cm^{-1} correspond to stretching vibration of $\text{C}-\text{O}$ Stretching. Peak observed at 610 cm^{-1} corresponds to stretching vibration of $\text{Ti}-\text{O}-\text{Ti}$. When the temperature of calcined increase from 200°C to 400°C show the reduction of unrelated peak of $\text{C} \equiv \text{C}$ stretching, $\text{C}=\text{C}=\text{C}$ stretching, $\text{C}=\text{O}$ bond, $\text{H}-\text{O}-\text{CH}_2$, $\text{H}-\text{O}-\text{H}$ bending of absorbed water and $\text{C}-\text{O}$ stretching. Moreover, TiO_2 catalyst calcined at

500°C show clearly characteristic absorptions of O-H and Ti-O-Ti Stretching due to complex compounds are decomposed with high calcination temperature [48-50].

From Figure 21, TGA of TiO₂ catalyst before calcination conform with the FT-IR spectrum. The increasing of calcination temperature will decrease weight of TiO₂ catalyst. From TGA, weight of TiO₂ catalyst stable at temperature above 500 °C. According to TGA and FT-IR spectrum, increasing of calcination temperature will decrease H₂O and other compound such as C=C=C, C-O and etc. The result from TGA and FT-IR show that below 300 °C TiO₂ catalyst was a complex of TiO₂.



Figure 20 Fourier transform infrared spectroscopy (FT-IR) of all TiO₂ catalysts prepared by sol-gel method.

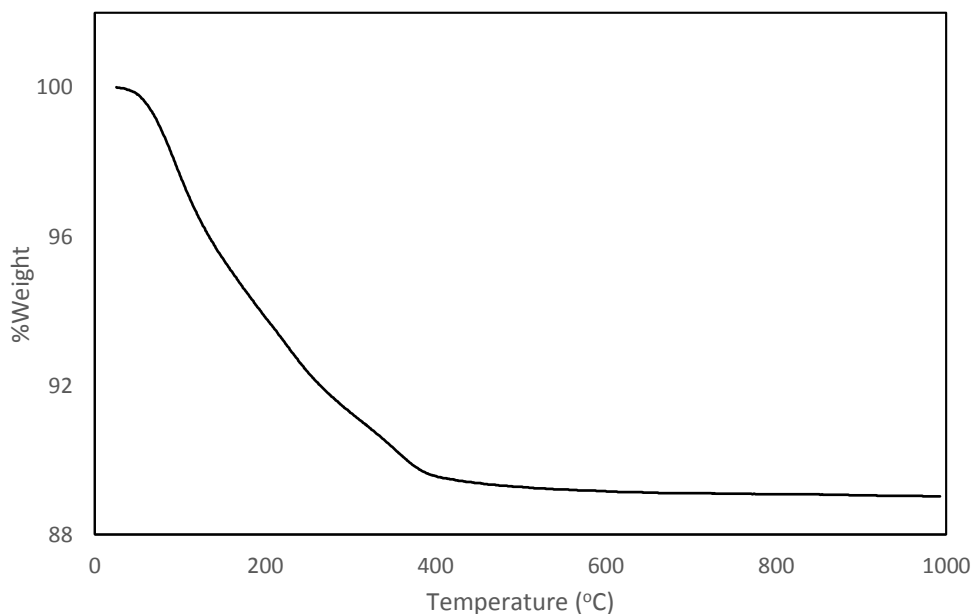


Figure 21 Thermal gravimetric analysis (TGA) of gel TiO₂ (TiO₂ catalyst before calcination).

Figure 22 and Figure 23 show that TiO₂ catalyst have more crystallinity give the less catalyst activity. Moreover, more surface area had more catalyst activity because larger surface area implies higher number of active site. According to Figure 24, catalytic activity was a function of reaction time. The long reaction time give high catalytic activity. [2, 6]

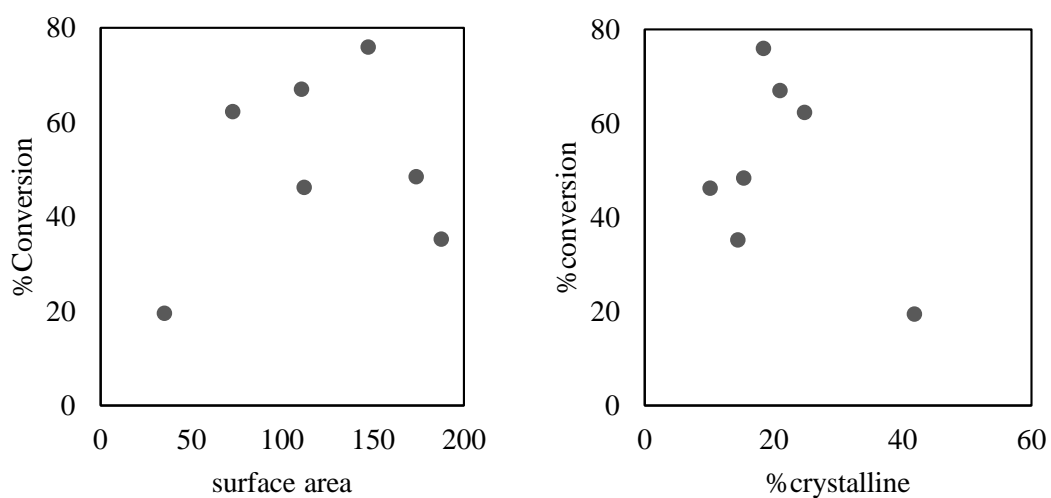


Figure 22 %Conversion with surface area and %crystalline of TiO₂ catalysts.

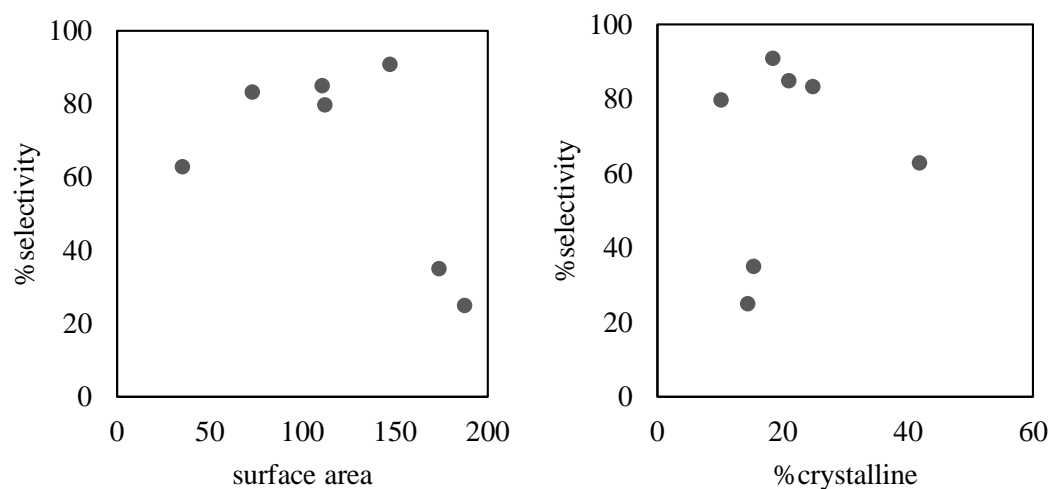


Figure 23 %Selectivity with surface area and %crystalline of TiO_2 catalysts.

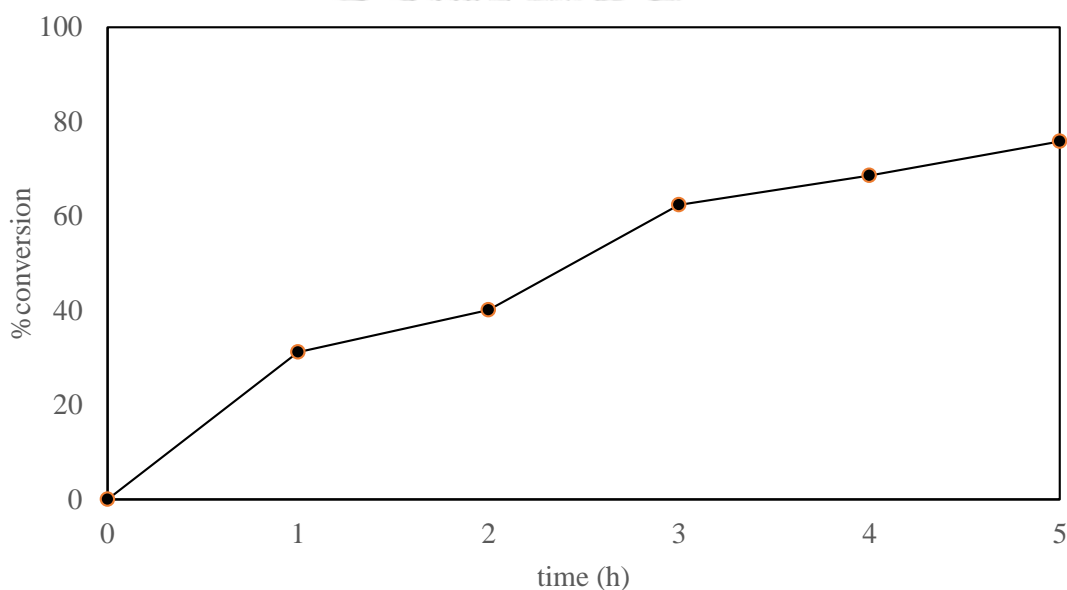


Figure 24 %Conversion of TiO_2 catalyst calcination at 300°C as a function of time.

The highest conversion and selectivity of epoxidation reaction of TiO_2 catalysts was TiO_2 catalyst calcination at 300°C . Therefore, TiO_2 catalyst calcination at 300°C was interesting for testing with reaction time and reused catalyst. According to Figure 24, conversion of TiO_2 catalyst calcination at 300°C was a function of reaction time. The increasing of reaction time for 5 h. increase the conversion of epoxidation reaction.

According to Figure 25 and Figure 26, both conversion and selectivity of TiO_2 catalyst calcination at 300°C decrease with increase run of epoxidation reaction.

Moreover, conversion of epoxidation reaction was slightly decrease as a function of run of epoxidation reaction. However, selectivity of epoxidation reaction significantly decreases with run of epoxidation reaction.

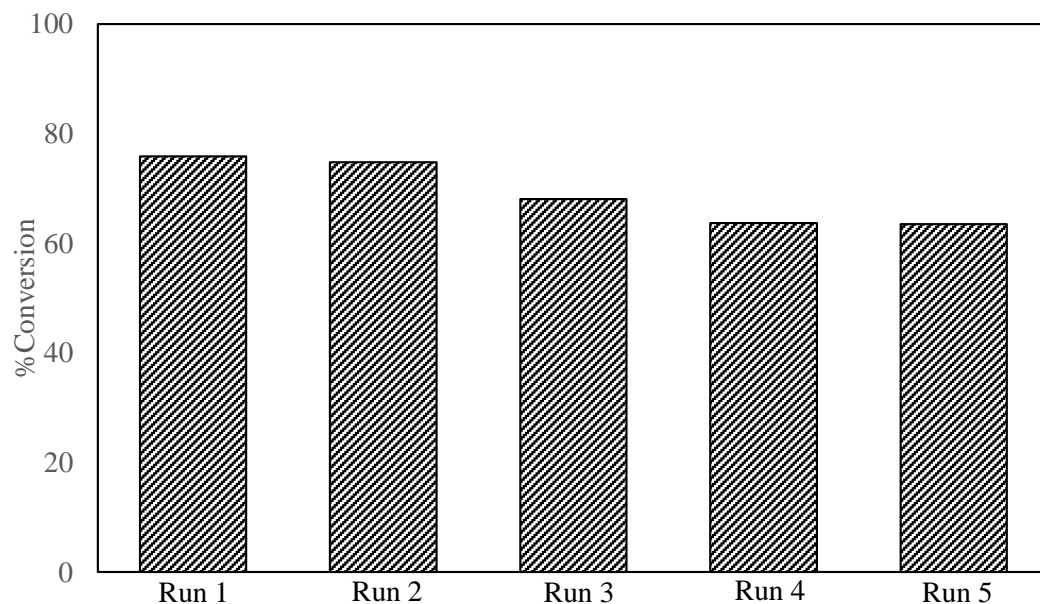


Figure 25 Conversion of reuse TiO_2 catalyst calcination temperature at 300°C at 5 h.

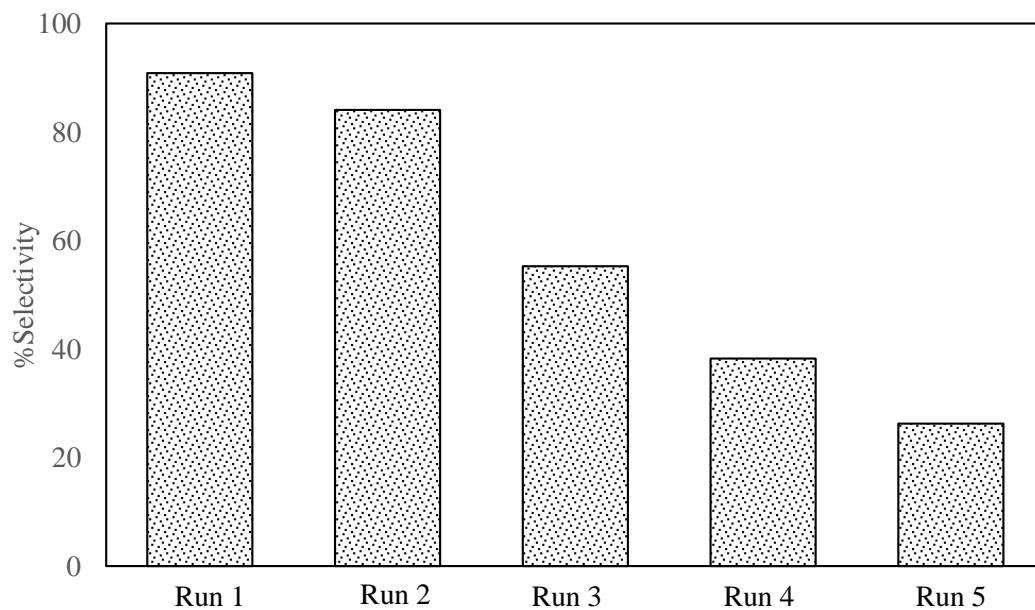


Figure 26 Selectivity of reuse TiO_2 catalyst calcination temperature at 300°C at 5 h.

4.2. Epoxidation of $\text{TiO}_2/\text{SiO}_2$ catalysts with different SiO_2 supported

4.2.1. Catalytic activity and selectivity of $\text{TiO}_2/\text{SiO}_2$ catalyst with different SiO_2 supported.

The result of TiO_2 catalyst found that more crystallinity gave less conversion and more surface area causes more conversion. Therefore, SiO_2 support is interesting for this reaction because SiO_2 support gave less crystallinity and high surface area. According to **Figure 27**, $\text{TiO}_2/\text{Silicalite}$ gave the highest conversion which gave 44.4% conversion at 5h. However, $\text{TiO}_2/\text{Silica gel}$ gave the lowest conversion with 5% conversion at 5h. $\text{TiO}_2/\text{fumed-SiO}_2$, $\text{TiO}_2/\text{MCM-41}$, and $\text{TiO}_2/\text{SBA-15}$ gave same conversion around 16% conversion at 5h. The selectivity of epoxidation in **Figure 28** shows that no epoxidation reaction when using $\text{TiO}_2/\text{silica-gel}$. However, $\text{TiO}_2/\text{silicalite}$ gave lower selectivity than $\text{TiO}_2/\text{MCM-41}$, fumed SiO_2 and SBA-15.

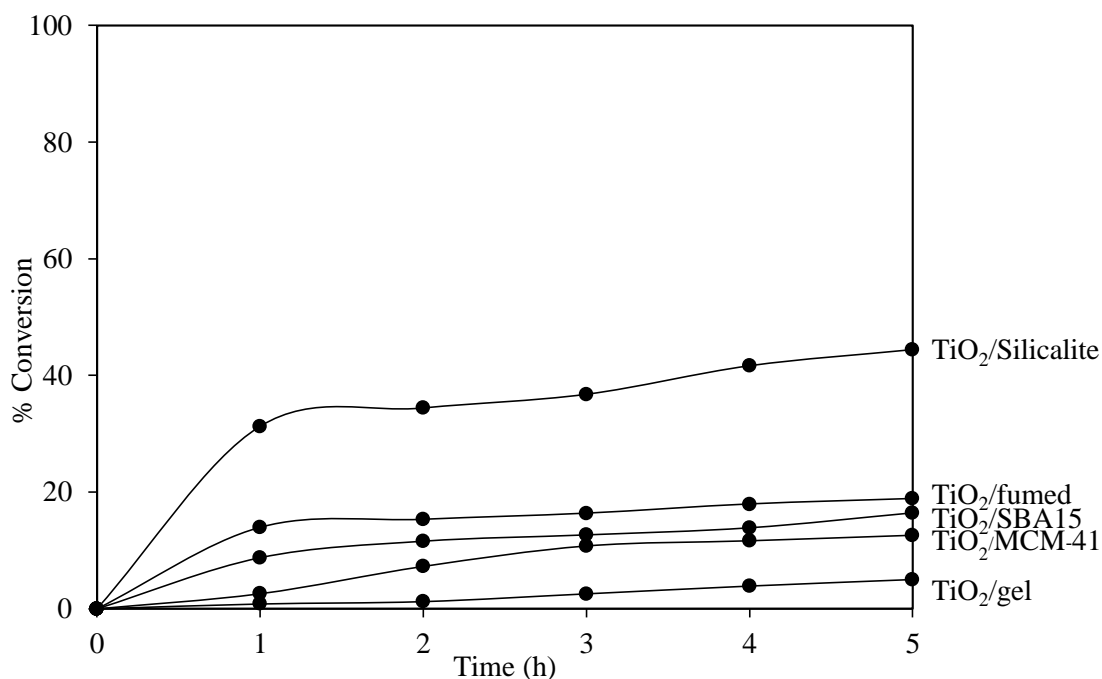


Figure 27 Catalytic activity of all $\text{TiO}_2/\text{SiO}_2$ catalysts in epoxidation of methyl oleate.

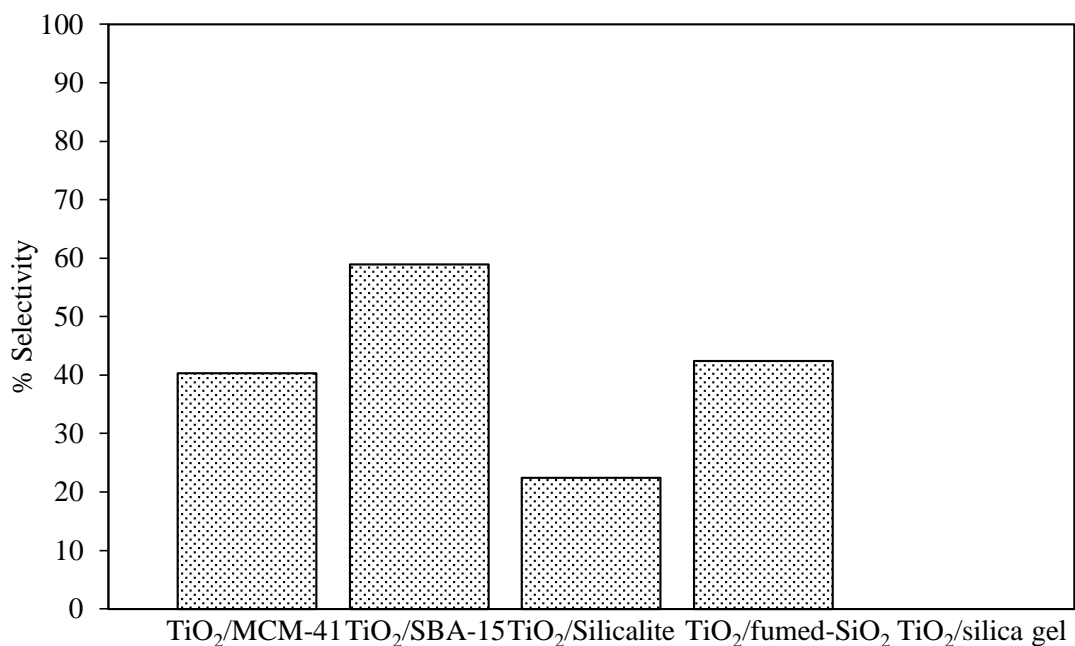


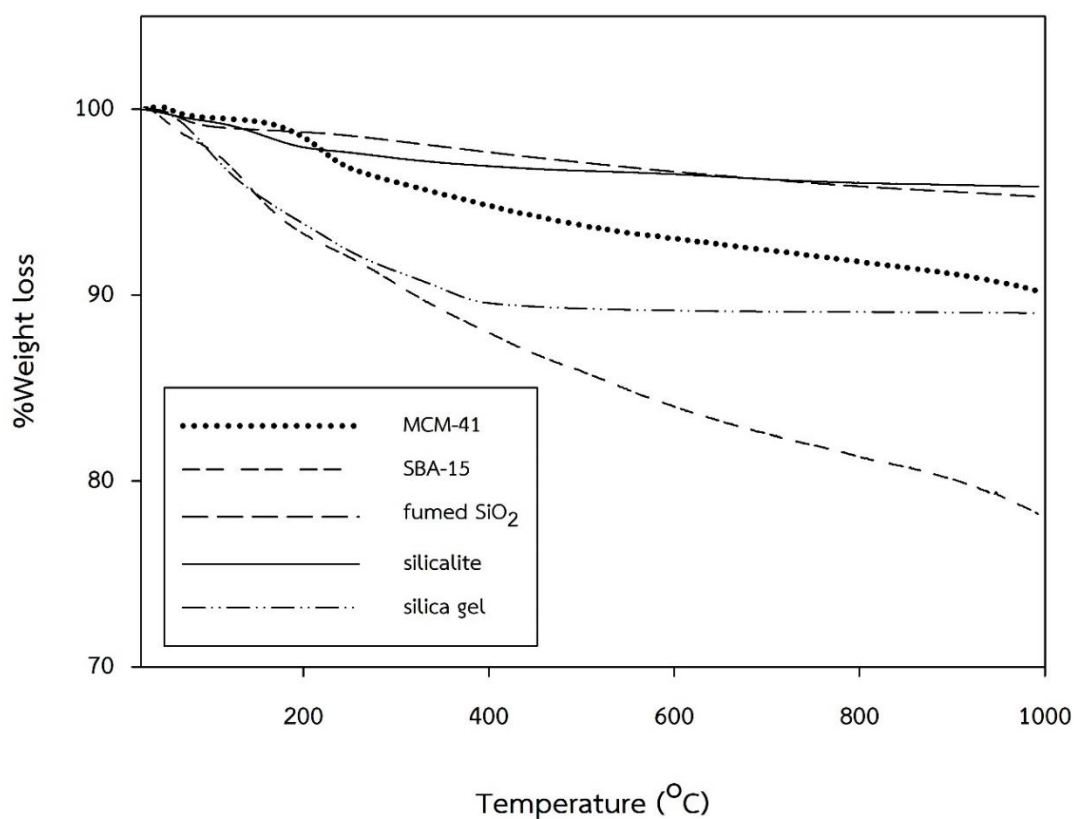
Figure 28 Selectivity of all TiO₂/SiO₂ catalyst in epoxidation of methyl oleate at 5 h.

4.2.2. Characterization of TiO₂/SiO₂ catalyst with different SiO₂ supported

The thermal gravimetric analysis result show in Table 17 and Figure 29. According to Table 17, different SiO₂ support was adsorbed different amount of H₂O. As show in Figure 29, TiO₂/silicagel show constant weight at 400°C. However, weight of TiO₂/SBA-15, MCM-41, silicalite and fumed SiO₂ decrease along the increase of temperature. Moreover, TiO₂/SBA-15 show the highest H₂O adsorbed at 21.65 wt% H₂O. Therefore, TiO₂/SBA-15 give higher selectivity than other silica support. Due to lower amount of H₂O, which can occur the ring opening. The more H₂O adsorbed make the less side reaction. H₂O adsorbed of silicalite, fumed SiO₂ are the same but the selectivity of fumes SiO₂ was higher than silicalite. According to the smaller pore mouth of silicalite, which make longer reaction. That lead to ring opening of epoxide.

Table 17 H₂O adsorbed by Thermal gravimetric analysis (TGA).

Catalyst	wt% H ₂ O adsorbed
TiO ₂ /Silicalite	4.11
TiO ₂ /fumed SiO ₂	4.7
TiO ₂ /SBA 15	21.65
TiO ₂ /MCM 41	9.84
TiO ₂ /Silica gel	10.95

Figure 29 Thermal gravimetric analysis (TGA) of TiO₂/SiO₂ with different support.

According to Figure 30, all catalyst has different size of support. However, both fumed-silica and silicalite gave a little bit different in SEM between SiO₂ supported and TiO₂/SiO₂. All-silica support gave sphere morphology. However, fumed-SiO₂ showed larger size of catalyst than both SiO₂-gel and Silicalite. The smallest catalyst was

silicalite. Thus, silicalite gave the highest surface area. Therefore, silicalite gave the highest catalyst activity. From SEM-EDX, found that Ti is well dispersed for all $\text{TiO}_2/\text{SiO}_2$. $\text{TiO}_2/\text{fumed-SiO}_2$ was represented as a characteristic of $\text{TiO}_2/\text{MCM-41}$ and $\text{TiO}_2/\text{SBA-15}$. Due to same catalyst activity and selectivity of $\text{TiO}_2/\text{fumed-SiO}_2$, $\text{TiO}_2/\text{MCM-41}$, and $\text{TiO}_2/\text{SBA-15}$. The same Ti wt. % loading of TIP gave difference catalytic activity. According to **Table 18**, the highest catalytic activity is $\text{TiO}_2/\text{Silicalite}$, which gave 31.26% conversion at 1 h. The lowest catalytic activity is $\text{TiO}_2/\text{Silica gel}$ with 0.83% conversion at 1 h. However, the highest Ti wt. % at surface is $\text{TiO}_2/\text{Silica gel}$. The lowest Ti wt. % at surface are $\text{TiO}_2/\text{fumed-silica}$, $\text{TiO}_2/\text{SBA-15}$ and $\text{TiO}_2/\text{MCM-41}$. Therefore, the Ti wt. % at surface of the same TIP concentration did not affect catalyst activity and selectivity. High Ti wt. % at surface of catalyst gave high catalyst activity. However, $\text{TiO}_2/\text{silica-gel}$ gave low catalyst activity because of high Ti wt. % at surface[20]. On the other hand, high Ti wt. % at surface of catalyst gave low selectivity of epoxide.

Table 18 Conversion of $\text{TiO}_2/\text{SiO}_2$ catalyst and composition of each TiO_2 species at catalyst surface.

Catalyst	Conversion (%, at 5 h)	Selectivity (%, at 5 h)	Ti (wt.%) ^a
$\text{TiO}_2/\text{Silicalite}$	44.41	22.38	5.91 ± 1.60
$\text{TiO}_2/\text{fumed SiO}_2$	18.86	42.44	1.13 ± 0.35
$\text{TiO}_2/\text{SBA 15}$	16.40	58.90	1.25 ± 0.20
$\text{TiO}_2/\text{MCM 41}$	12.56	40.26	1.36 ± 0.23
$\text{TiO}_2/\text{Silica gel}$	0.83	0	9.21 ± 0.52

^a Ti wt.% from SEM-EDX

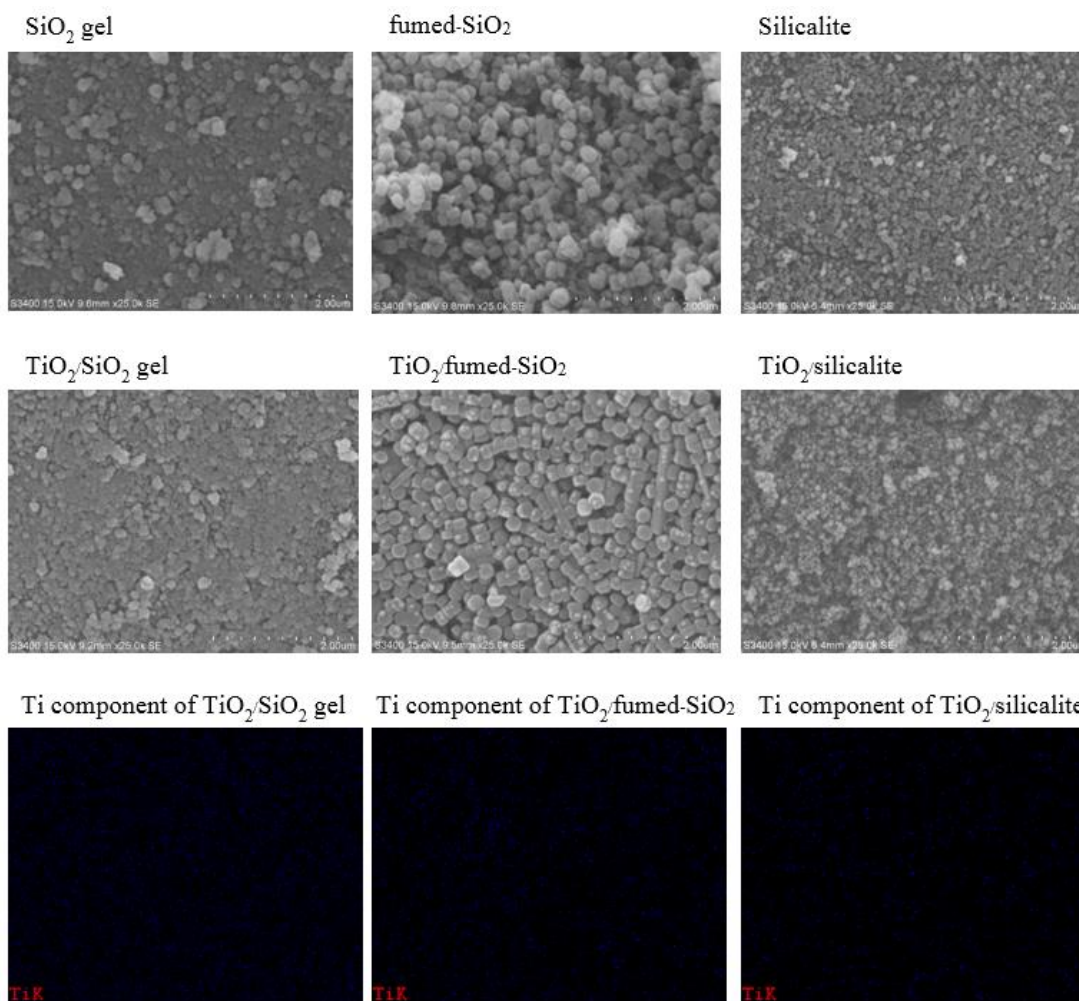


Figure 30 Scanning electron microscopy (SEM) and Energy dispersive x-ray spectroscopy (EDX) results of TiO₂/SiO₂ catalyst.

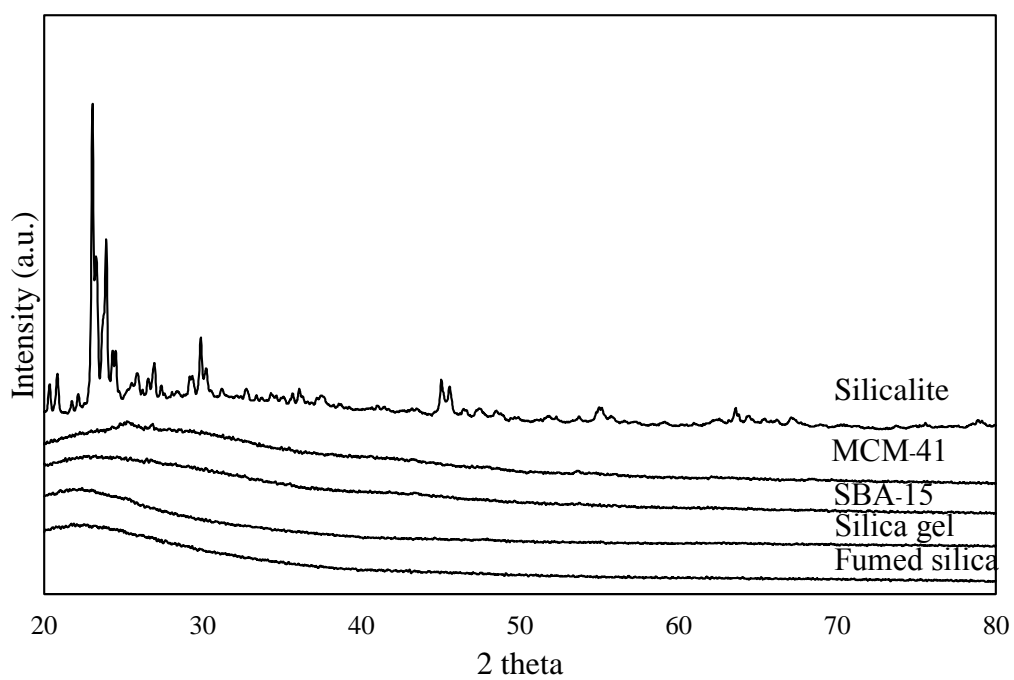


Figure 31 X-ray diffraction (XRD) of $\text{TiO}_2/\text{SiO}_2$ catalysts.

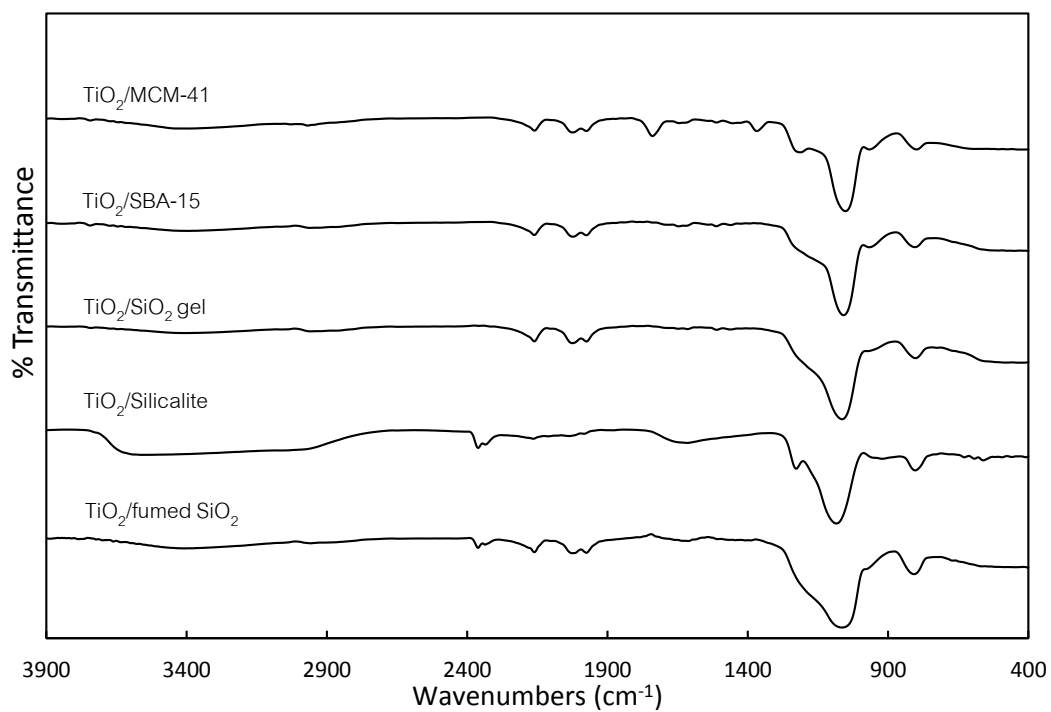


Figure 32 Fourier transform infrared spectroscopy (FT-IR) of $\text{TiO}_2/\text{SiO}_2$ with different SiO_2 support.

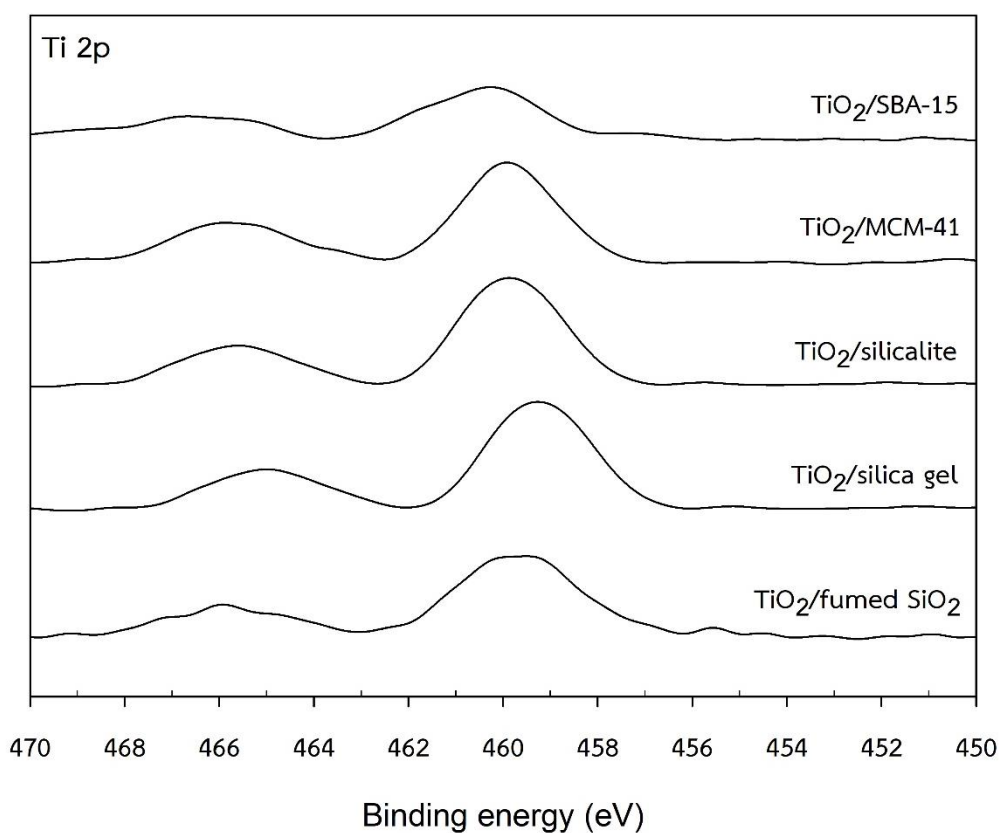


Figure 33 X-ray photoelectron spectroscopy (XPS) of TiO₂/SiO₂ with different support.

The difference of all SiO₂ support is their silinol group and crystalline at surface. From XRD pattern in **Figure 31**, silicalite shows different XRD pattern from other silica support. Silicalite shows single reflection at $2\theta = 23^\circ$, which indicates monoclinic (silicalite) [8]. However, all TiO₂/SiO₂ catalyst did not show the reflection at $2\theta = 25.3$, which is characteristic for crystalline TiO₂ in anatase phase because of low Ti% loading.

Figure 32 shows the FT-IR spectra of TiO₂/SiO₂ catalyst. In the spectrum of TiO₂/Silicalite catalyst, there are several characteristic absorptions: Peak observed at 3780 cm⁻¹ corresponds to Si-OH stretching of silanols and H-bonded Si-OH stretching of surface hydroxyl. Peak observed at 3500 – 3100 cm⁻¹ 1730 and 1610 cm⁻¹ corresponds to stretching and bending modes of adsorbed water molecules. Peak observed at 2970 cm⁻¹ correspond to stretching vibration of weak OH stretching. Peak observed at 2160 and 2020 cm⁻¹ correspond to overtone modes of silica frame. Peak

observed at 1065 and 970 cm^{-1} corresponds to Si–O stretching region at higher frequencies. Peak observed at 798 cm^{-1} correspond to O–H bending mode of hydrogen bonded. [51, 52]. Since Ti wt.% loading of TIP was 1.5%. Then all several characteristic absorptions peaks of Ti–O stretching were blocked out by SiO_2 support. However, small characteristic peak at 960 cm^{-1} was indicated that difference type of Ti stretching such as Ti bonds with the SiO_4 group ($\text{Si-O}\cdots\text{Ti}$), titanol groups (Ti=O), Si–O bond within the $\text{O}\cdots\text{H}$ groups, Ti–O bond within TiO_4 tetrahedra and SiO O bonds within defective SiOH sites (OH) Ti [42, 53].

The chemical state of Ti and the typical specimen spectra of Ti 2p were investigated by XPS measurement. According to **Figure 33**, all $\text{TiO}_2/\text{SiO}_2$ catalysts showed two main peaks of Ti, which binding energies at 466.3 eV and 459.5 eV for Ti 2p_{1/2} and Ti 2p_{3/2}, respectively. The XPS peaks at 466.3 eV for Ti 2p_{1/2} and 459.5 eV for Ti 2p_{3/2} are corresponded to Ti^{4+} . [43, 54] MCM-41, silicalite, and silica gel show a strong peak at both 466.3 eV and 459.5 eV than SBA-15 and fumed SiO_2 .

According to **Figure 34** and **Table 19**, the only silicalite was microporous material with type I and type II isotherm (p/p_0 more than 0.9). Other SiO_2 support were mesoporous material with type IV isotherm with H1 hysteresis loop [8, 14]. The more wt% of H_2O adsorbed gave more % selectivity of methyl oleate epoxide. However, silicalite which are microporous material give less selectivity, due to the effect of pore size.

Figure 35, shows that tetrahedral coordination was increased with increasing of selectivity of methyl oleate epoxide. However, all $\text{TiO}_2/\text{SiO}_2$ catalysts show wavelength around 220 nm, which be a TiO_2 with tetrahedral. On the other hand, SiO_2 -gel give wavelength around 259 nm, which be a TiO_2 with 5 or 6 coordination. The TiO_2 with tetrahedral coordinate was the active size of epoxidation reaction. Therefore, TiO_2 with SBA-15 catalyst give the highest selectivity and TiO_2 with SiO_2 – gel give lowest selectivity.[2, 8, 14]

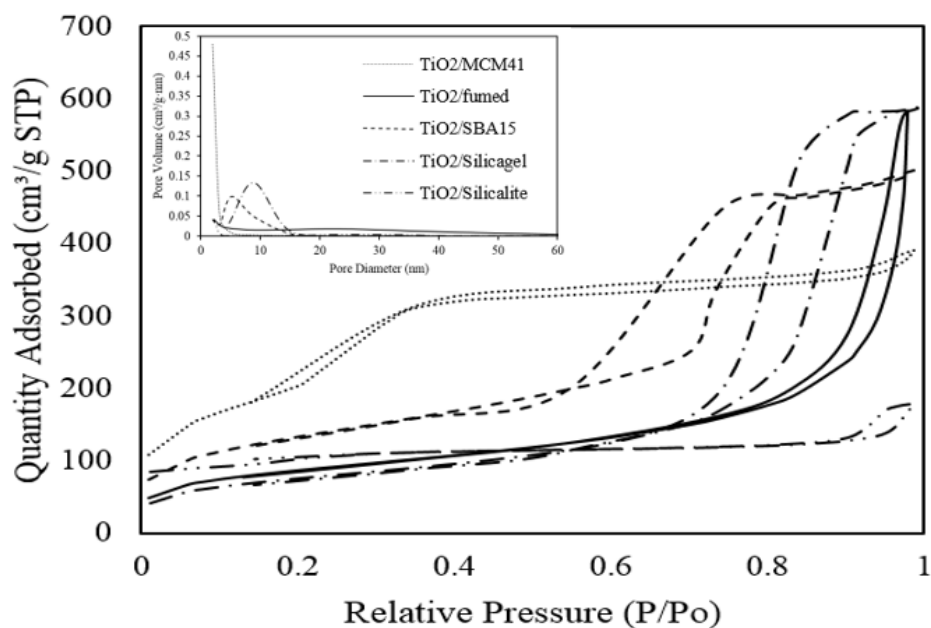


Figure 34 N_2 physisorption of TiO_2 with different SiO_2 supports

Table 19 Effect of pore size and Wt% H_2O adsorbed to selectivity of TiO_2/SiO_2 support.

Catalyst	Pore size (nm)	Wt% H_2O adsorbed	%Selectivity (5 h.)
$TiO_2/Silicalite$	N/A	4.11	22.38
$TiO_2/Fumed\ silica$	11.5	4.7	42.44
$TiO_2/SBA-15$	5.2	21.65	58.90
$TiO_2/MCM-41$	2.4	9.84	40.26
$TiO_2/Silica\ gel$	8.6	10.95	0

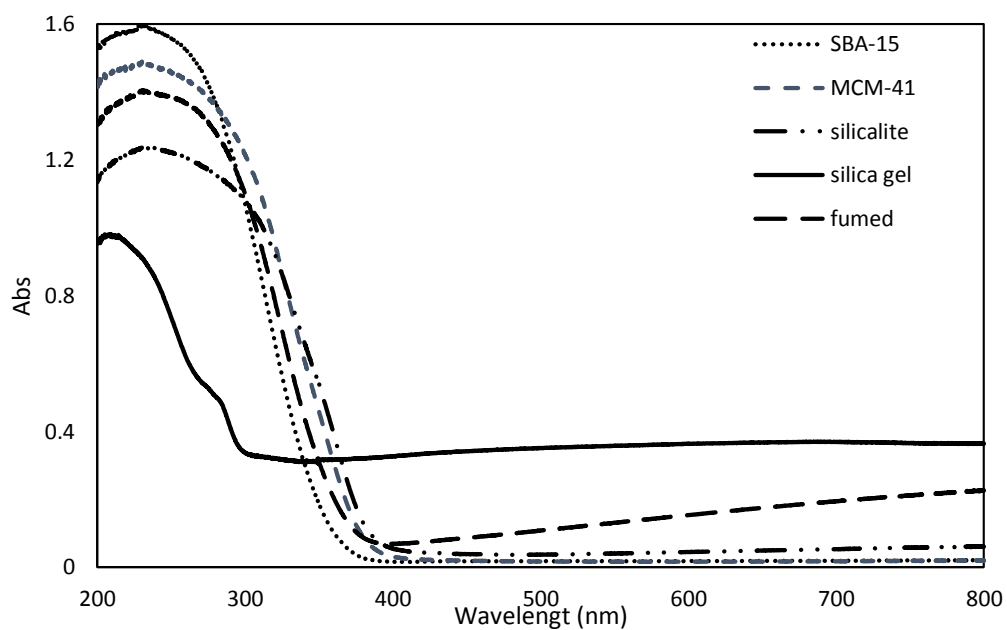


Figure 35 UV-vis of TiO_2 with different SiO_2 supports

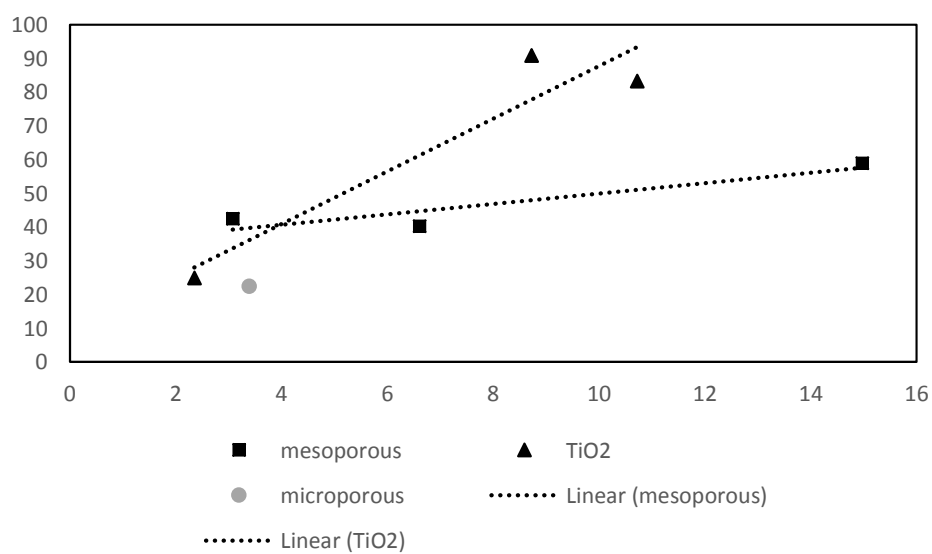


Figure 36 wt% H_2O adsorbed and selectivity of all catalysts

According to Figure 36, the more H_2O adsorbed give the more selectivity of epoxidation. However, pore size of catalysts also effects to selectivity. Non-porous

material gives higher selectivity than porous material. However, microporous give the less selectivity.

4.3. Epoxidation of $\text{TiO}_2/\text{SiO}_2$ catalysts by different synthesis method

4.3.1. Catalytic activity and selectivity of $\text{TiO}_2/\text{SiO}_2$ catalysts by different synthesis method.

After, we had selected fumed- SiO_2 as a supported. However, there are several synthesis methods for $\text{TiO}_2/\text{SiO}_2$ catalysts. Therefore, the different methods of $\text{TiO}_2/\text{SiO}_2$ were interesting. In this part, three different interested synthesis methods were incipient wetness impregnation, wet impregnation and grafting method. Catalytic activity from three different methods of $\text{TiO}_2/\text{SiO}_2$ for epoxidation reaction of methyl oleate with hydrogen peroxide show in **Figure 37**. The catalytic activity of those three different synthesis methods was increased with reaction time. The catalytic activity of the reactions using the catalysts synthesis from wet impregnation, incipient wetness impregnation and grafting methods at 5 h were 35.21% , 38.23% and 38.52% , respectively. This result showed similar catalytic activity of the three different catalyst synthesis.

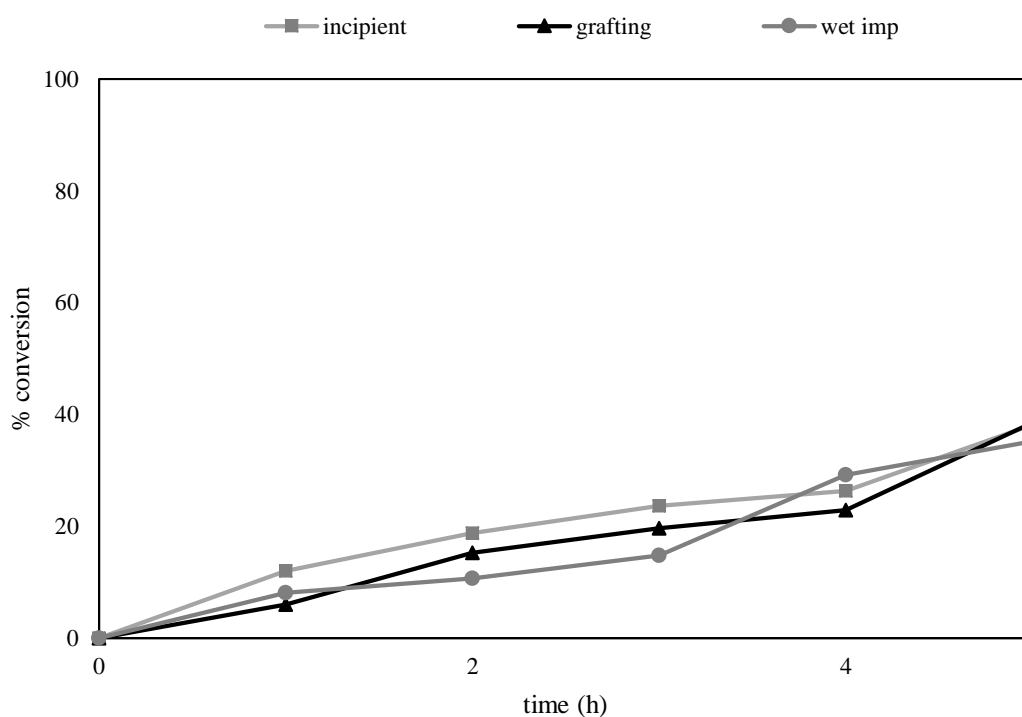


Figure 37 Catalytic activity of $\text{TiO}_2/\text{SiO}_2$ different synthesis methods.

According to Figure 38, the highest selectivity of $\text{TiO}_2/\text{SiO}_2$ by three different synthesis methods was $\text{TiO}_2/\text{SiO}_2$ catalyst that synthesis by wet impregnation method (28%). On the other hand, the other $\text{TiO}_2/\text{SiO}_2$ catalyst using incipient wetness impregnation (13%) and grafting method (15%) gave similar selectivity of methyl oleate epoxide. Therefore, the best catalyst synthesis method was wet impregnation. However, incipient wetness impregnation is the quickest way to synthesis $\text{TiO}_2/\text{SiO}_2$ catalyst.

4.3.2. Characterization of $\text{TiO}_2/\text{SiO}_2$ by different synthesis method

According to Figure 39, SEM micrographs of fumed silica support (Figure 39 A), $\text{TiO}_2/\text{fumed-SiO}_2$ by incipient wetness impregnation (Figure 39 B), $\text{TiO}_2/\text{fumed-SiO}_2$ by grafting (Figure 39 C) and $\text{TiO}_2/\text{fumed-SiO}_2$ by wet impregnation (Figure 39D) show similar small sphere particles morphology. The surface of catalyst from SEM-EDX show

in Table 20, the result showed that the wet impregnation method gave highest Ti wt% . According to Table 20, single point surface area of $\text{TiO}_2/\text{SiO}_2$ catalyst showed that the incipient wetness impregnation gave the highest surface area ($312 \text{ m}^2/\text{g}$). However, surface area of $\text{TiO}_2/\text{SiO}_2$ from three different synthesis method are not difference ($273\text{-}312 \text{ m}^2/\text{g}$). Moreover, surface area, Ti wt% and surface morphology did not affect to catalytic activity. However, the Ti wt% had an effect on catalyst selectivity. The highest Ti wt% gave highest selectivity.

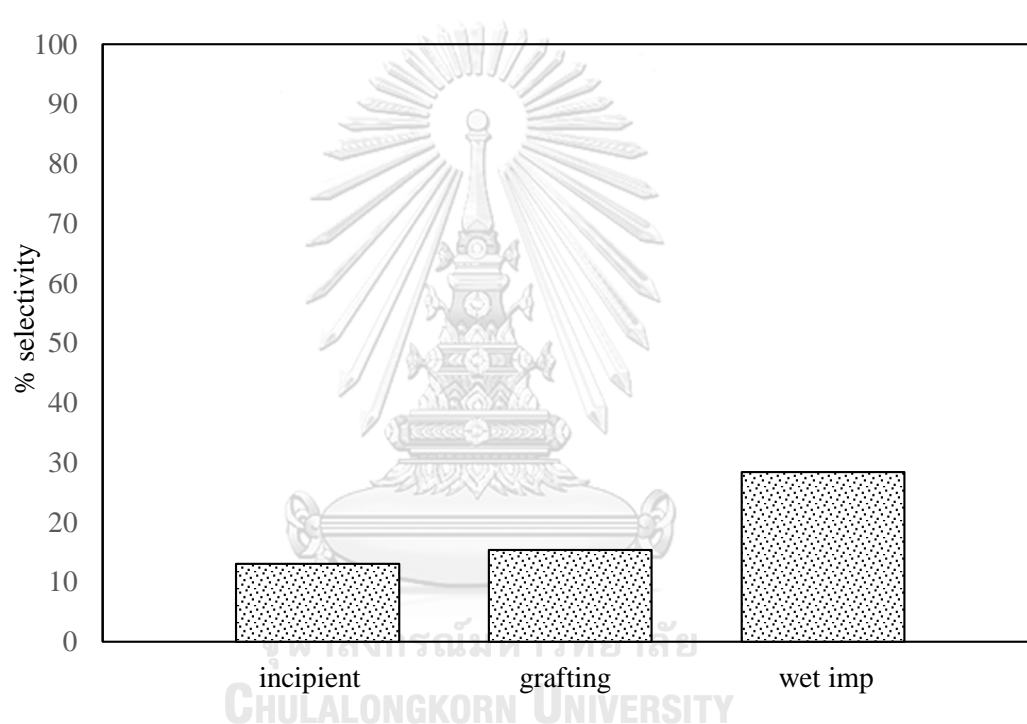


Figure 38 Selectivity of $\text{TiO}_2/\text{SiO}_2$ different synthesis methods.

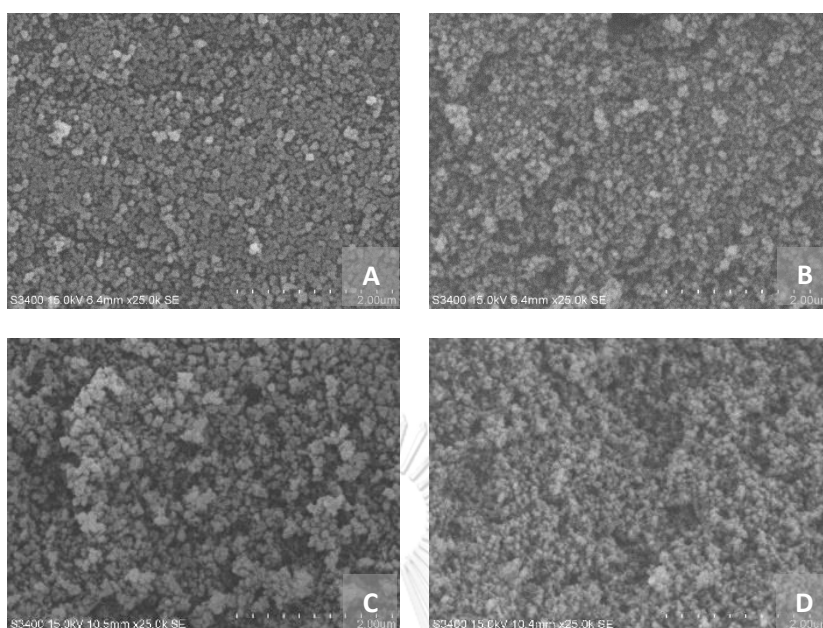


Figure 39 SEM micrographs of A) fumed silica support, B) $\text{TiO}_2/\text{SiO}_2$ by incipient wetness impregnation, C) $\text{TiO}_2/\text{SiO}_2$ by grafting and D) $\text{TiO}_2/\text{SiO}_2$ by wet impregnation.

Table 20 Wt% of Ti on $\text{TiO}_2/\text{SiO}_2$ surface from SEM-EDX analysis and surface area from N_2 physisorption analysis.

method	Ti wt%	Surface area (m^2/g)	Conversion (at 5 h)
Incipient wetness impregnation	1.78	312	38.23%
grafting	1.55	273	38.52%
Wet impregnation	3.41	304	35.21%

According to Figure 40, the XRD of three different $\text{TiO}_2/\text{SiO}_2$ catalyst synthesis showed strong reflection around $2\Theta = 22$, attributing to the amorphous SiO_2 . No significant TiO_2 peak intensity was observed, which the characteristic peak of crystalline titanium dioxide (TiO_2) in the anatase phase is reflect around $2\Theta = 25.40$, probably due to low TiO_2 loading (around 1.5% Ti). In addition, no characteristic peaks either in

anatase or rutile phases of TiO_2 crystalline were observed at the TiO_2 loading range of 1-15 wt%. [8, 11, 55]

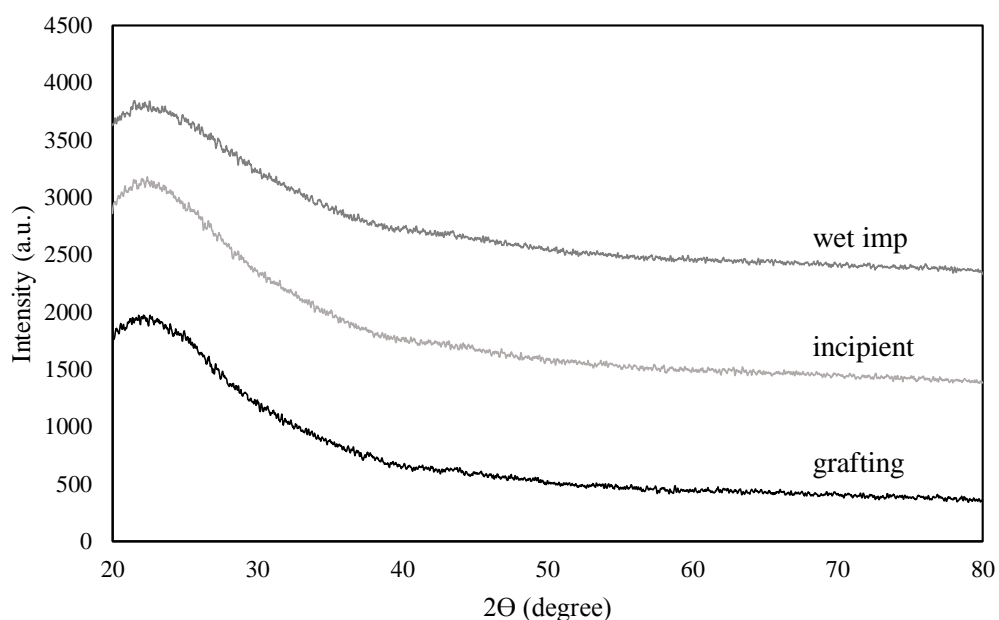


Figure 40 X-ray diffraction patterns of $\text{TiO}_2/\text{SiO}_2$ by wet impregnation, incipient wetness impregnation and grafting method.

The UV-Vis spectra of $\text{TiO}_2/\text{SiO}_2$ of three different catalysts were compared in Figure 41. Nature and coordination geometry of Ti were characterized by UV-Vis spectra. Isolated tetrahedral Ti oxide coordination shows a typical band below 250 nm. The peak around 210 nm was assigned to the ligand-to-metal charge-transfer (LMCT) transition of the isolated Ti oxide monomer with tetrahedral coordination. The results from UV-Vis spectra show that those three $\text{TiO}_2/\text{SiO}_2$ catalysts had Ti oxide with tetrahedral coordination. No band centered at 260-300 nm and near 330 nm, which indicated the absence of the hexacoordinated Ti species and anatase phase, respectively. $\text{TiO}_2/\text{SiO}_2$ by wet impregnation has higher intensity of Ti due to high Ti wt% [2, 8, 11, 15, 21, 56]. The results are selectivity of epoxidation follow by Ti wt% of catalyst and the different synthesis method give the same catalytic activity. Therefore, the interesting $\text{TiO}_2/\text{SiO}_2$ catalyst effect was %Ti loading.

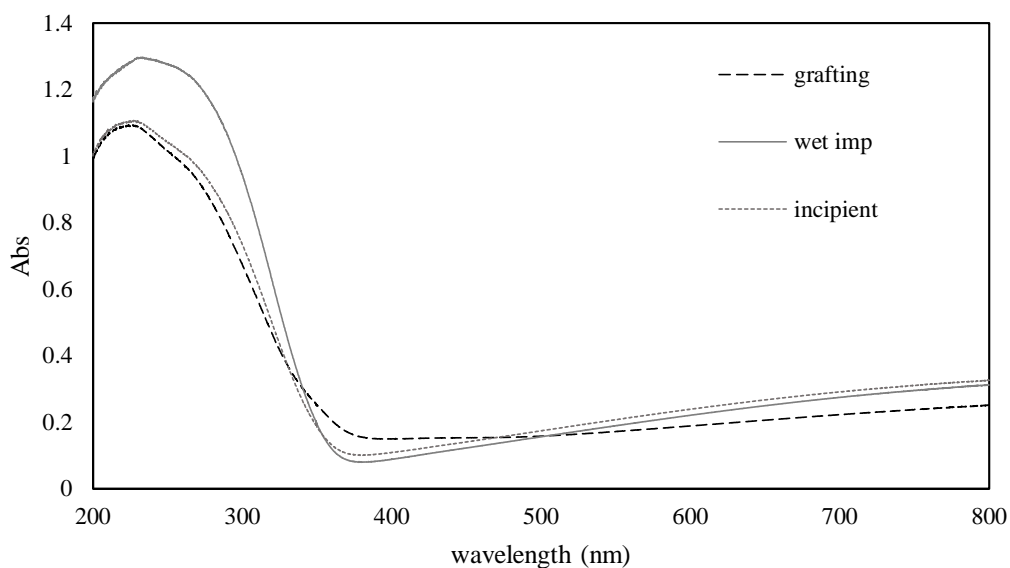


Figure 41 UV-Vis spectra of $\text{TiO}_2/\text{SiO}_2$ by wet impregnation, incipient wetness impregnation and grafting method.

4.4. Epoxidation of $\text{TiO}_2/\text{SiO}_2$ catalysts with different %Ti loading

4.4.1. Catalytic activity and selectivity of $\text{TiO}_2/\text{SiO}_2$ catalysts with different %Ti loading

According to Figure 42 and Figure 43, the catalytic activity and selectivity of epoxidation reaction of methyl oleate are a function of %Ti loading. For catalytic activity, the more % Ti loading give more catalytic activity of epoxidation reaction. Moreover, increase % Ti from 1.5% to 15% Ti loading increase catalytic activity from 18.86% to 97.49% conversion. However, the more %Ti loading give less epoxide from epoxidation reaction. Which increase % Ti loading from 1.5% to 15% decrease selectivity of epoxidation reaction from 42.44% to 0.00% selectivity. Therefore, the more %Ti loading give more catalytic activity but less selectivity of epoxidation reaction.

The Ti leaching of $\text{TiO}_2/\text{SiO}_2$ of 2.5% Ti loading were interested because of high catalytic activity and selectivity of epoxidation reaction. The catalytic activity and selectivity of Ti leaching show in Figure 44 and Figure 45 respectively. The catalytic activity and selectivity of $\text{TiO}_2/\text{SiO}_2$ catalyst slightly decrease as a function of reuse catalyst. The catalytic activity was decrease from 29.51% to 15.47% conversion with

increase number of reuse catalyst. The selectivity of epoxidation reaction was decrease from 20.76% to 7.53% selectivity with increase number of reuse catalyst.

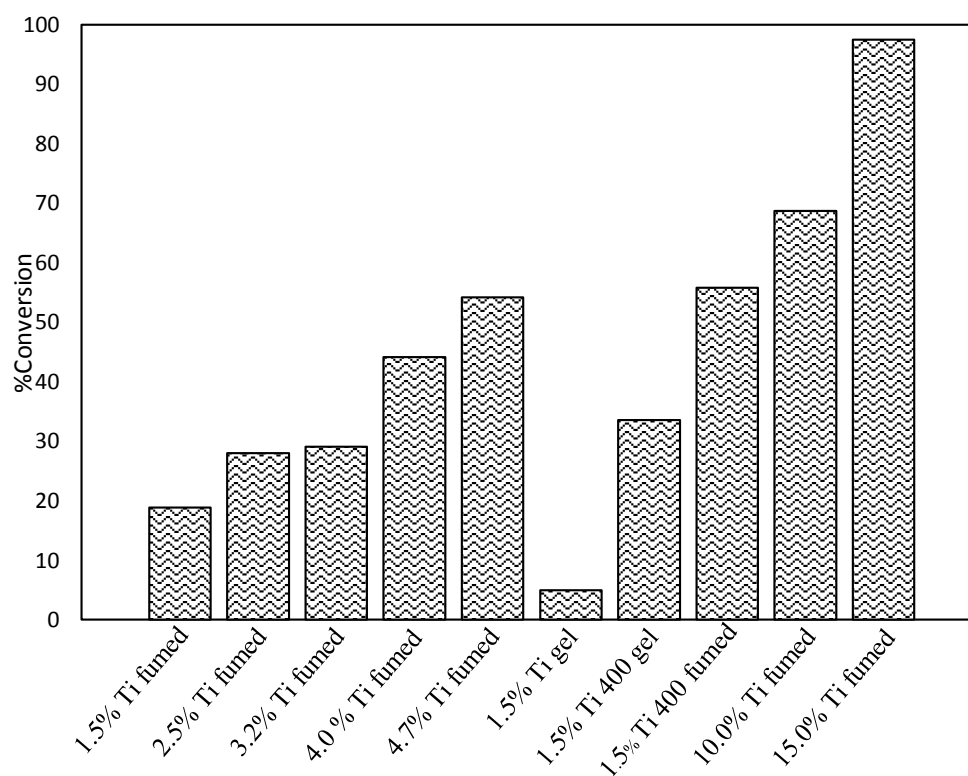


Figure 42 Catalytic activity of $\text{TiO}_2/\text{SiO}_2$ catalysts with different %Ti loading.

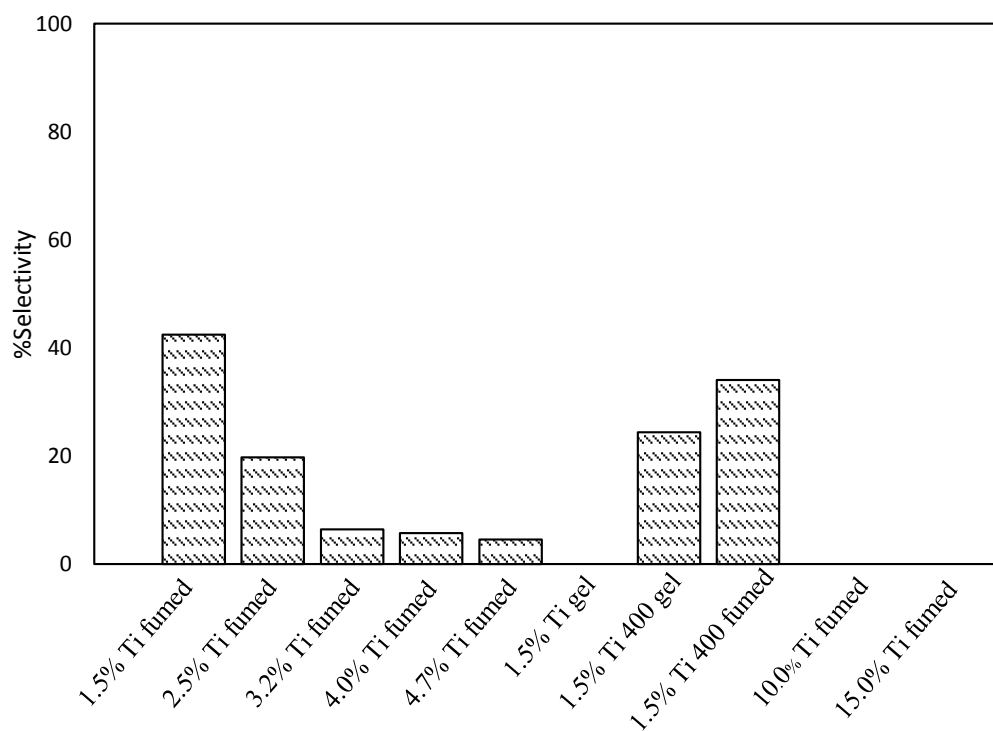


Figure 43 Selectivity of $\text{TiO}_2/\text{SiO}_2$ catalysts with different %Ti loading.

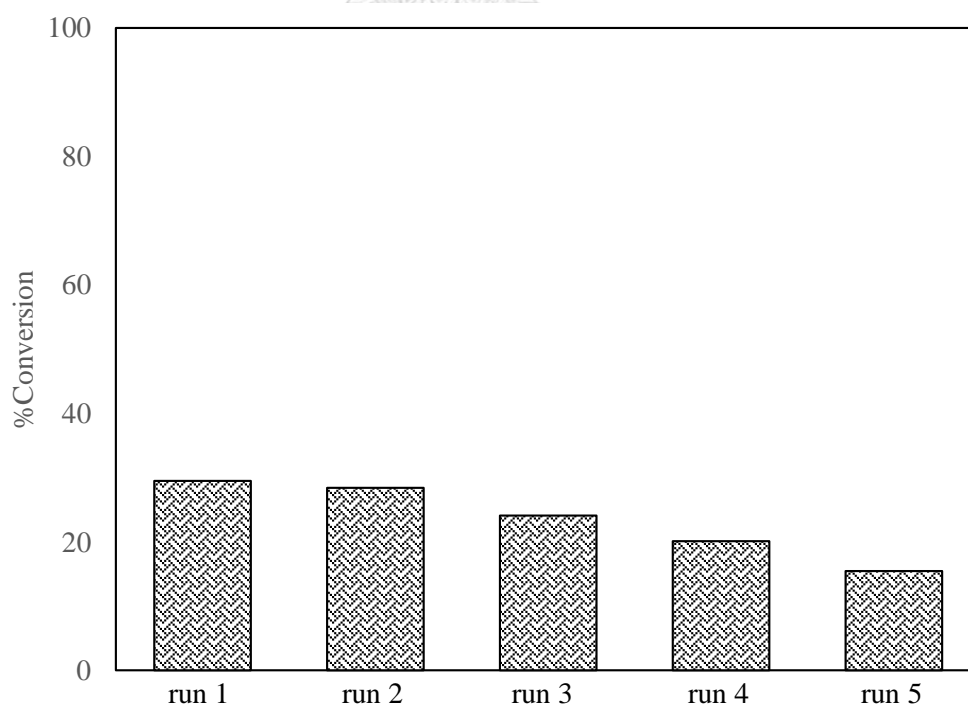


Figure 44 Conversion of $\text{TiO}_2/\text{SiO}_2$ catalysts with different %Ti loading.

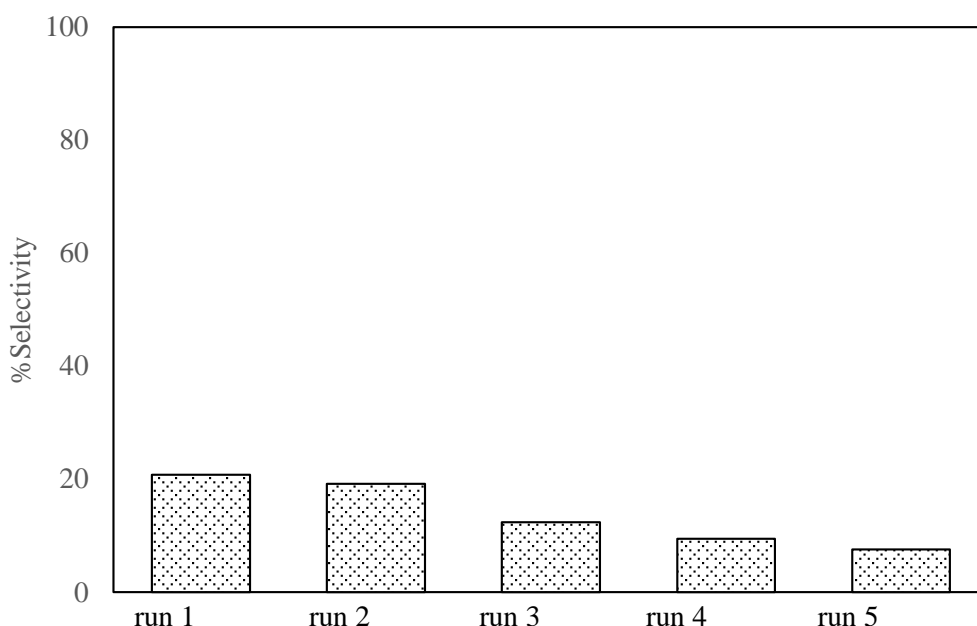


Figure 45 Selectivity of $\text{TiO}_2/\text{SiO}_2$ catalysts with different %Ti loading.

4.4.2. Characterization of $\text{TiO}_2/\text{SiO}_2$ catalysts with different %Ti loading

According to Figure 46, X-ray diffraction of $\text{TiO}_2/\text{SiO}_2$ catalysts with different %Ti loading show same result of the diffraction peaks at %Ti below 4.0%. At 4.7% Ti loading, anatase phase appeared, which peaks $2\theta = 25.3^\circ, 37.8^\circ, 48.1^\circ, 54.0^\circ$ and 55.1° . At low Ti loading, TiO_2 species were highly dispersed on the silica surface. Therefore, TiO_2 species exist in highly dispersed on silica surface at Ti loading below 4.7%. The intensity of anatase phase increase with the increase of Ti loading. The bulk crystalline TiO_2 formed above the monolayer of surface TiO_2 . The bulk crystalline TiO_2 could physically blocked the pour mouths of $\text{TiO}_2/\text{SiO}_2$ catalyst leading to the increase of crystallinity of $\text{TiO}_2/\text{SiO}_2$ catalyst. Therefore, the more Ti loading give the more catalytic activity but the less selectivity of epoxidation reaction. Due to, high crystallinity of high Ti loading on $\text{TiO}_2/\text{SiO}_2$ catalyst lead to low selectivity but high conversion.

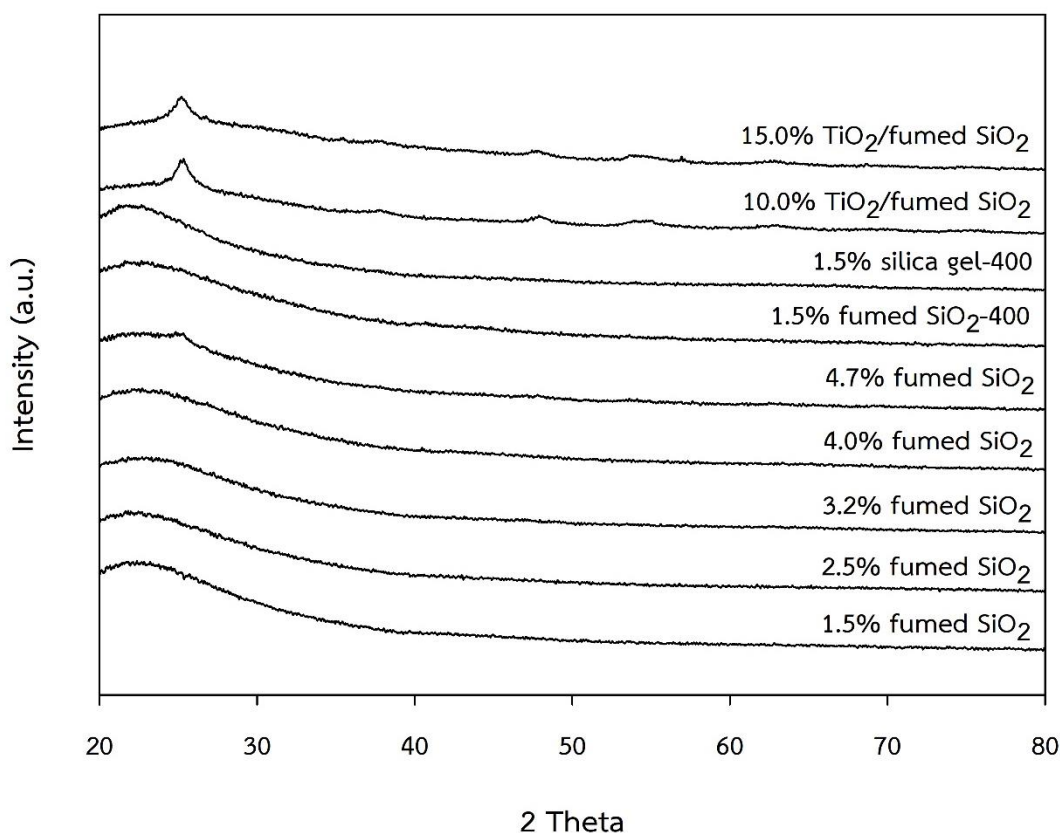


Figure 46 X-ray diffraction (XRD) of $\text{TiO}_2/\text{SiO}_2$ catalysts with different %Ti loading.

According to Figure 47, fourier transform infrared spectra of all catalysts revealed a small characteristic peak at approximately 960 cm^{-1} was indicated that difference type of Ti stretching such as Ti bonds with the SiO_4 group ($\text{Si-O}\cdots\text{Ti}$), titanol groups (Ti=O), Si-O bond within the $\text{O}\cdots\text{H}$ groups, Ti-O bond within TiO_4 tetrahedra and SiO O bonds within defective SiOH sites (OH) Ti [42, 53]. Furthermore, these bands were more intense reasonable from the Ti content in its structure of supports. On the other hand, the characteristics band at ≈ 1081 related to the antisymmetric stretching vibration and changes in Si-O-Si deformation.

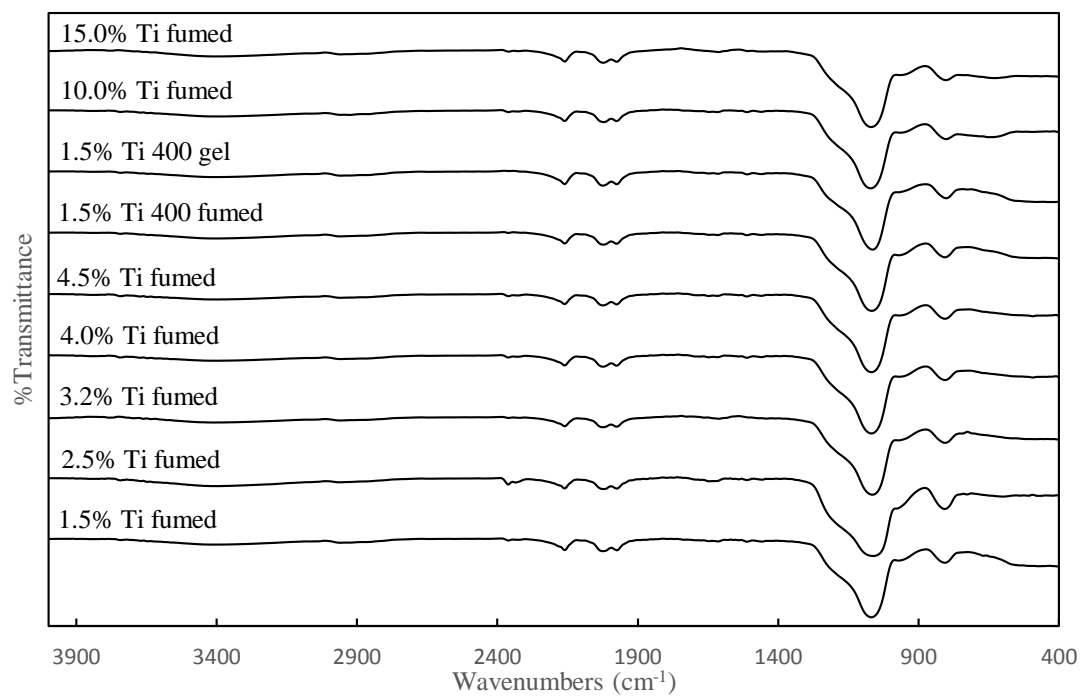


Figure 47 Fourier transform infrared spectroscopy (FT-IR) of TiO₂/SiO₂ with different %Ti loading.



CHAPTER V

CONCLUSIONS AND RECOMMENDATIONS

5.1 Conclusions

TiO₂ catalyst shows that the more crystallinity gave the less catalyst activity. The commercial TiO₂ type B has less crystallinity. Therefore, the commercial TiO₂ type B gave higher catalytic activity than the commercial TiO₂ type A. At high calcination temperature, anatase phase is not stable and sintering occurred. Therefore, at 500°C TiO₂ gave less anatase phase, more crystallinity and less surface area than another TiO₂ catalyst. Since, larger surface area implies higher number of active site. Thus, 500°C showed lower catalytic activity than 300°C and 200°C TiO₂ catalyst. However, TiO₂ at 100°C and 200°C calcination temperature showed a complex compound. Which not form TiO₂. Therefore, 100°C and 200°C TiO₂ catalyst gave lower conversion and selectivity than another TiO₂ catalyst.

Since, crystallinity and surface area affect to catalyst activity of epoxidation of methyl oleate, then SiO₂ support are interesting. Those five differences of SiO₂ supported gave different catalytic activity and selectivity. The highest catalytic activity is TiO₂/silicalite because of their specific silanols group and higher Ti wt.% at surface. The highest selectivity is TiO₂/SBA-15. Due to strong absorptions of H₂O, which lead to low side reaction. TiO₂/fumed SiO₂ gave higher selectivity than silicalite and MCM-41 because of bigger pore mouth than MCM-41 and silicalite.

Fumed SiO₂ gave high catalytic activity and selectivity. Therefore, the study of synthesis method of TiO₂/SiO₂ used fumed SiO₂ as a support. Those three different synthesis method gave the same catalytic activity. However, TiO₂/SiO₂ synthesis by wet impregnation gave higher selectivity due to high Ti wt%.

Ti loading affect to both catalytic activity and selectivity. Therefore, the study of Ti loading was important. The result is the more Ti loading gave the more catalytic activity. However, the more Ti loading gave the less selectivity. Due to, more side reaction occurred at high Ti loading.

5.2 Recommendations

1. The effects of amount of catalysts, temperature and drop of hydrogen peroxide should be investigated in the next researches.
2. The further study of commercial catalysts for epoxidation reaction of biodiesel should be researches.
3. Effect of Ti loading to selectivity of epoxidation reaction.



REFERENCES

- [1] N.K. Sarina Grinberg, Charles Linder, Victoria Kolot and Eliahu Heldman, Asymmetric bolaamphiphiles from vernonia oil designed for drug delivery, *Eur. J. Lipid Sci. Technol.*, 112 (2010).
- [2] N. Wilde, C. Worch, W. Suprun, R. Gläser, Epoxidation of biodiesel with hydrogen peroxide over Ti-containing silicate catalysts, *Microporous and Mesoporous Materials*, 164 (2012) 182-189.
- [3] S.N. Federico Galli, Carlo Pirola, Claudia L. Bianchi, Epoxy Methyl Soyate as Bio-Plasticizer: Two Different Preparation Strategies, *CHEMICAL ENGINEERING TRANSACTIONS*, 37 (2014).
- [4] U. Biermann, U. Bornscheuer, M.A. Meier, J.O. Metzger, H.J. Schafer, Oils and fats as renewable raw materials in chemistry, *Angew Chem Int Ed Engl*, 50 (2011) 3854-3871.
- [5] Y.-B. Huang, M.-Y. Yao, P.-P. Xin, M.-C. Zhou, T. Yang, H. Pan, Influence of alkenyl structures on the epoxidation of unsaturated fatty acid methyl esters and vegetable oils, *RSC Advances*, 5 (2015) 74783-74789.
- [6] M. Guidotti, R. Psaro, N. Ravasio, M. Sgobba, E. Gianotti, S. Grinberg, Titanium–Silica Catalysts for the Production of Fully Epoxidised Fatty Acid Methyl Esters, *Catalysis Letters*, 122 (2007) 53-56.
- [7] D.R. Lehnen, R. Guzzato, D. Defferrari, L.L. Albornoz, D. Samios, Solvent-free biodiesel epoxidation, *Environmental Chemistry Letters*, 12 (2013) 335-340.
- [8] N. Wilde, M. Pelz, S.G. Gebhardt, R. Gläser, Highly efficient nano-sized TS-1 with micro-/mesoporosity from desilication and recrystallization for the epoxidation of biodiesel with H₂O₂, *Green Chemistry*, 17 (2015) 3378-3389.
- [9] Z. Li, Y. Zhao, S. Yan, X. Wang, M. Kang, J. Wang, H. Xiang, Catalytic Synthesis of Carbonated Soybean Oil, *Catalysis Letters*, 123 (2008) 246-251.
- [10] V.B. Borugadda, V.V. Goud, Epoxidation of Castor Oil Fatty Acid Methyl Esters (COFAME) as a Lubricant base Stock Using Heterogeneous Ion-exchange Resin (IR-120) as a Catalyst, *Energy Procedia*, 54 (2014) 75-84.

- [11] Y. Wei, G. Li, Q. Lü, C. Cheng, H. Guo, Green and efficient epoxidation of methyl oleate over hierarchical TS-1, *Chinese Journal of Catalysis*, 39 (2018) 964-972.
- [12] M. -Y. Yao, Y. -B. Huang, X. Niu, H. Pan, Highly Efficient Silica-Supported Peroxycarboxylic Acid for the Epoxidation of Unsaturated Fatty Acid Methyl Esters and Vegetable Oils, *ACS Sustainable Chemistry & Engineering*, 4 (2016) 3840-3849.
- [13] R. Turco, C. Pischetola, R. Tesser, S. Andini, M. Di Serio, New findings on soybean and methylester epoxidation with alumina as the catalyst, *RSC Advances*, 6 (2016) 31647-31652.
- [14] V. Smeets, L. Ben Mustapha, J. Schnee, E. M. Gaigneaux, D. P. Debecker, Mesoporous SiO₂-TiO₂ epoxidation catalysts: Tuning surface polarity to improve performance in the presence of water, *Molecular Catalysis*, 452 (2018) 123-128.
- [15] T. Kamegawa, N. Suzuki, M. Che, H. Yamashita, Synthesis and unique catalytic performance of single-site Ti-containing hierarchical macroporous silica with mesoporous frameworks, *Langmuir*, 27 (2011) 2873-2879.
- [16] Y. Zhang, C. Xia, M. Lin, Q. Duan, B. Zhu, X. Peng, B. Wang, S. Yuan, Y. Liu, X. Shu, Sponge-structured titanasilicate zeolite with high catalytic activity in epoxidation of fatty acid methyl ester, *Catalysis Communications*, 101 (2017) 1-4.
- [17] Y. Leng, J. Zhao, P. Jiang, J. Wang, Amphiphilic polyoxometalate-paired polymer coated Fe₃O₄: magnetically recyclable catalyst for epoxidation of bio-derived olefins with H₂O₂, *ACS Appl Mater Interfaces*, 6 (2014) 5947-5954.
- [18] E. Poli, N. Bion, J. Barrault, S. Casciato, V. Dubois, Y. Pouilloux, J.-M. Clacens, Selective epoxidation of unsaturated fatty esters over peroxophosphotungstic catalysts (POW) under solvent free conditions: Study of the POW catalyst's mechanism, *Catalysis Today*, 157 (2010) 371-377.
- [19] T.R. Amarante, P. Neves, A.A. Valente, F.A. Paz, A.N. Fitch, M. Pillinger, I.S. Goncalves, Hydrothermal synthesis, crystal structure, and catalytic potential of a one-dimensional molybdenum oxide/bipyridinedicarboxylate hybrid, *Inorg Chem*, 52 (2013) 4618-4628.
- [20] X. Yang, X. Ma, S. Wang, J. Gong, Transesterification of dimethyl oxalate with phenol

over TiO₂/SiO₂: Catalyst screening and reaction optimization, *AIChE Journal*, 54 (2008) 3260-3272.

[21] M. Cozzolino, M. Di Serio, R. Tesser, E. Santacesaria, Grafting of titanium alkoxides on high-surface SiO₂ support: An advanced technique for the preparation of nanostructured TiO₂/SiO₂ catalysts, *Applied Catalysis A: General*, 325 (2007) 256-262.

[22] M.J. Ramos, C.M. Fernandez, A. Casas, L. Rodriguez, A. Perez, Influence of fatty acid composition of raw materials on biodiesel properties, *Bioresour Technol*, 100 (2009) 261-268.

[23] B. K. Sharma, K. M. Doll, S. Z. Erhan, Ester hydroxy derivatives of methyl oleate: tribological, oxidation and low temperature properties, *Bioresour Technol*, 99 (2008) 7333-7340.

[24] G. Fogassy, P. Ke, F. Figueras, P. Cassagnau, S. Rouzeau, V. Courault, G. Gelbard, C. Pinel, Catalyzed ring opening of epoxides: Application to bioplasticizers synthesis, *Applied Catalysis A: General*, 393 (2011) 1-8.

[25] E.D. WILLIAM R. SCHMITZ and JOHN G. WALLACE, N.F. E. I. Du Pont de Nemours and Company Inc., New York, Epoxidation of Methyl Oleate with Hydrogen Peroxide, *THE JOURNAL OF THE AMERICAN OIL CHEMIST'S SOCIETY*, 31 (1954) 3.

[26] M.S. H. C. WOHLERS, and . P. LeVAN, A.C.C. Solvay Process Division, Syracuse, N. Y., Yield in Epoxidation Reactions, *INDUSTRIAL AND ENGINEERING CHEMISTRY*, 50 (1958) 2.

[27] A. Nishimura, G. Mitsui, K. Nakamura, M. Hirota, E. Hu, Reforming Characteristics under Visible Light Response of Cr- or Ag-Doped Prepared by Sol-Gel and Dip-Coating Process, *International Journal of Photoenergy*, 2012 (2012) 1-12.

[28] L. Yu, J. He, C. Huang, M. Li, Y. Zhang, X. Zhou, H. Zhu, Electron transportation path build for superior photoelectrochemical performance of Ag₃PO₄/TiO₂, *RSC Advances*, 7 (2017) 54485-54490.

[29] U. Diebold, The surface science of titanium dioxide, *Surface Science Reports*, 48 (2003) 53-229.

[30] A. Fujishima, X. Zhang, Titanium dioxide photocatalysis: present situation and future

approaches, *Comptes Rendus Chimie*, 9 (2006) 750-760.

[31] D. Regonini, C. R. Bowen, A. Jaroenworuluck, R. Stevens, A review of growth mechanism, structure and crystallinity of anodized TiO₂ nanotubes, *Materials Science and Engineering: R: Reports*, 74 (2013) 377-406.

[32] U. Diebold, The surface science of titanium dioxide, *surface science reports*, 48 (2003) 53-229.

[33] D. P. Macwan, P. N. Dave, S. Chaturvedi, A review on nano-TiO₂ sol-gel type syntheses and its applications, *Journal of Materials Science*, 46 (2011) 3669-3686.

[34] A. Romeiro, D. Freitas, M. Emilia Azenha, M. Canle, H. D. Burrows, Effect of the calcination temperature on the photocatalytic efficiency of acidic sol-gel synthesized TiO₂ nanoparticles in the degradation of alprazolam, *Photochem Photobiol Sci*, 16 (2017) 935-945.

[35] C. -S. Kim, B. K. Moon, J. -H. Park, S. Tae Chung, S. -M. Son, Synthesis of nanocrystalline TiO₂ in toluene by a solvothermal route, *Journal of Crystal Growth*, 254 (2003) 405-410.

[36] H. Wu, J. Ma, C. Zhang, H. He, Effect of TiO₂ calcination temperature on the photocatalytic oxidation of gaseous NH₃, *Journal of Environmental Sciences*, 26 (2014) 673-682.

[37] Y. Chen, D. D. Dionysiou, Effect of calcination temperature on the photocatalytic activity and adhesion of TiO₂ films prepared by the P-25 powder-modified sol-gel method, *Journal of Molecular Catalysis A: Chemical*, 244 (2006) 73-82.

[38] N. Venkatachalam, M. Palanichamy, V. Murugesan, Sol-gel preparation and characterization of nanosize TiO₂: Its photocatalytic performance, *Materials Chemistry and Physics*, 104 (2007) 454-459.

[39] R.S. Devi, D.R. Venckatesh, D.R. Sivaraj, Synthesis of Titanium Dioxide Nanoparticles by Sol-Gel Technique, *International Journal of Innovative Research in Science, Engineering and Technology*, 03 (2014) 15206-15211.

[40] D.A.R. Richard L. Brutchey, Lars K. Andersen, and, T.D. Tilley, Influence of surface modification of Ti-SBA15 catalysts on the epoxidation mechanism for cyclohexene with

aqueous hydrogen peroxide, *Langmuir*, 21 (2005) 9576-9583.

[41] A. Wróblewska, P. Miądlicki, J. Tołpa, J. Sreńscek-Nazzal, Z. C. Koren, B. Michalkiewicz, Influence of the Titanium Content in the Ti-MCM-41 Catalyst on the Course of the α -Pinene Isomerization Process, *Catalysts*, 9 (2019).

[42] S.G. Sanches, J.H. Flores, M.I.P. da Silva, Ti dispersion on SBA-15 porous host to enhance photocatalytic hydrogen production, *Journal of Molecular Structure*, 1170 (2018) 9-17.

[43] H. Zhang, X. Shi, A. Tian, L. Wang, C. Liu, Electrochemical properties of Ti³⁺ doped Ag-Ti nanotube arrays coated with hydroxyapatite, *Applied Surface Science*, 436 (2018) 579-584.

[44] D. Mandelli, Y.N. Kozlov, W.A. Carvalho, G.B. Shul'pin, Oxidations by the system 'hydrogen peroxide-[Mn₂L₂O₃]²⁺ (L=1,4,7-trimethyl-1,4,7-triazacyclononane)-carboxylic acid', *Catalysis Communications*, 26 (2012) 93-97.

[45] Y. Kuwahara, N. Furuichi, H. Seki, H. Yamashita, One-pot synthesis of molybdenum oxide nanoparticles encapsulated in hollow silica spheres: an efficient and reusable catalyst for epoxidation of olefins, *Journal of Materials Chemistry A*, 5 (2017) 18518-18526.

[46] A. Rubinstein, R. Carmeli, R. Neumann, Formation of persulphate from sodium sulphite and molecular oxygen catalysed by H₅PV₂Mo₁₀O₄₀--aerobic epoxidation and hydrolysis, *Chem Commun (Camb)*, 50 (2014) 13247-13249.

[47] R. Turco, R. Vitiello, R. Tesser, A. Vergara, S. Andini, M. Di Serio, Niobium Based Catalysts for Methyl Oleate Epoxidation Reaction, *Topics in Catalysis*, 60 (2017) 1054-1061.

[48] M. Hema, A.Y. Arasi, P. Tamilselvi, R. Anbarasan, Titania Nanoparticles Synthesized by Sol-Gel Technique, *Chemical Science Transactions*, 2 (2012) 239-245.

[49] C.J. Huntley, K.D. Crews, M.L. Curry, Chemical Functionalization and Characterization of Cellulose Extracted from Wheat Straw Using Acid Hydrolysis Methodologies, *International Journal of Polymer Science*, 2015 (2015) 1-9.

[50] G. socrates, Infrared and Raman Characteristic Group Frequencies, JOHN WILEY&SONS, LTD, (2004).

- [51] H. Sanaeishoar, M. Sabbaghan, F. Mohave, Synthesis and characterization of micro-mesoporous MCM-41 using various ionic liquids as co-templates, *Microporous and Mesoporous Materials*, 217 (2015) 219-224.
- [52] A.S. Khan, H. Khalid, Z. Sarfraz, M. Khan, J. Iqbal, N. Muhammad, M.A. Fareed, I.U. Rehman, Vibrational spectroscopy of selective dental restorative materials, *Applied Spectroscopy Reviews*, 52 (2016) 507-540.
- [53] P. Devi, U. Das, A.K. Dalai, Production of glycerol carbonate using a novel Ti-SBA-15 catalyst, *Chemical Engineering Journal*, 346 (2018) 477-488.
- [54] M. Signoreto, E. Ghedini, V. Trevisan, C.L. Bianchi, M. Ongaro, G. Cruciani, TiO₂-MCM-41 for the photocatalytic abatement of NO_x in gas phase, *Applied Catalysis B: Environmental*, 95 (2010) 130-136.
- [55] X. Ren, G. Miao, Z. Xiao, F. Ye, Z. Li, H. Wang, J. Xiao, Catalytic adsorptive desulfurization of model diesel fuel using TiO₂/SBA-15 under mild conditions, *Fuel*, 174 (2016) 118-125.
- [56] J. J. a. T. D. Tilley, Silica-Supported, Single-Site Titanium Catalysts for Olefin Epoxidation. A Molecular Precursor Strategy for Control of Catalyst Structure, *J. AM. CHEM. SOC.*, 124 (2002).

APPENDICES

APPENDICES A: CALCULATION OF CRYSTALLITE SIZE

Calculation of the crystallite size by Debye-Scherrer equation

The crystallite size can be calculated from 2θ profile analysis, FWHM, by Debye-Scherrer equation (A.1) that was suitable for partial size below 100 nm.

Debye-Scherrer equation:

$$D = \frac{\kappa\lambda}{\beta\cos\theta} \quad (\text{A.1})$$

Where

D = Average size of the crystal (\AA)

κ = Dimensionless shape factor (0.9)

λ = The x-ray wavelength (1.54439 \AA for $\text{CuK}\alpha$)

β = The x-ray diffraction broadening (radian)

θ = Observed peak angle (degree)

The broadening of a single diffraction peak is the product of the crystallite dimensions in the direction perpendicular to the planes that produced the diffraction peak. The X-ray diffraction broadening can be obtained by using Warren's equation (A.2).

Warren's equation:

$$\beta^2 = \beta_M^2 - \beta_S^2$$
$$\beta = \sqrt{\beta_M^2 - \beta_S^2} \quad (\text{A.2})$$

Where

β_M = Measured peak width in radians at half peak height

β_S = Corresponding width of a standard material

Example : Calculation of the crystallite size of pure TiO₂ calcined at 400°C for two hours

The half-weight width (101) diffraction peak

$$\beta_M = 1.1295 \text{ degree}$$

$$\beta_M = 0.019713 \text{ radian}$$

The corresponding half-height width of peak of TiO₂

$$\beta_s = 0.00075 \text{ radian}$$

The pure width

$$\beta = \sqrt{\beta_M^2 - \beta_s^2}$$

$$\beta = \sqrt{0.019713^2 - 0.00075^2}$$

$$\beta = 0.019699 \text{ radian}$$

Where

$$\lambda = 1.01117 \text{ \AA}$$

$$\beta = 0.019699 \text{ radian}$$

$$2\theta = 25.3465 \text{ degree}$$

$$\theta = 12.6732 \text{ degree}$$

$$\begin{aligned} \text{The crystallite size (D)} &= \frac{0.9 \times 1.01117}{0.019699 \cos 12.6732} \\ &= 72.20 \text{ \AA} \\ &= 7.22 \text{ nm} \end{aligned}$$

APPENDICES B: CALCULATION OF WEIGHT FRACTION OF ANATASE, RUTILE AND BROOKITE PHASE OF TiO₂

Calculation of the weight fraction

The phase of TiO₂ can be calculated from the integrated intensities of peaks at 2θ of 25.3° was assigned to anatase TiO₂, whereas the peak at 27.4° corresponded to be rutile phase and the peak at 30.6° was associated to brookite.

The weight fraction of TiO₂ sample can be calculated as follows equation (B.1)-(B.3).

$$W_A = \frac{A_A}{A_A + A_B + A_R} \quad (B.1)$$

$$W_B = \frac{A_B}{A_A + A_B + A_R} \quad (B.2)$$

$$W_R = \frac{A_R}{A_A + A_B + A_R} \quad (B.3)$$

Where

W_A = Weight fraction of anatase phase TiO₂

W_B = Weight fraction of brookite phase TiO₂

W_R = Weight fraction of rutile phase TiO₂

A_A = The intensity of anatase peak

A_B = The intensity of brookite peak

A_R = The intensity of rutile peak

Example : Calculation of the phase contents TiO_2 calcined at 400°C for two hours

Where

The integrated intensities of anatase (A_A) = 742

The integrated intensities of brookite (A_B) = 73

The integrated intensities of rutile (A_R) = 141

The weight fraction of the phase content can be calculated by as follows:

$$W_A = \frac{742}{742+73+141} = 0.77$$

$$W_B = \frac{73}{742+73+141} = 0.09$$

$$W_R = \frac{141}{742+73+141} = 0.14$$

APPENDICES C: CALCULATION OF CATALYST PREPARATION

For TiO_2 / fumed SiO_2 by incipient wetness impregnation

Example: 12%TIP of TiO_2 / SiO_2 or 2.5% Ti of TiO_2 / SiO_2

Reagent:

absolute ethanol	100%
Titanium isopropoxide (TIP)	97%

Volume of absolute ethanol:

Fumed SiO_2 (pore volume)	$0.64 \text{ cm}^3/\text{g}$
5 g. of fumed SiO_2 contain	$0.64 \text{ cm}^3/\text{g} * 5 \text{ g}$
	3.2 cm^3 of solution
Constant TIP at	0.89 cm^3
Used of absolute ethanol	$3.2 - 0.89 \text{ cm}^3$
	2.31 cm^3

VITA

NAME Nichaphat Sangkanchanavanich

DATE OF BIRTH 27 November 1994

PLACE OF BIRTH Bangkok

INSTITUTIONS ATTENDED graduated high school from Mater Dei school in 2013.
graduated Bachelor's Degrees from faculty of Engineering in
Chemical Engineering, Kasetsart University, Bangkok,
Thailand in 2017.

HOME ADDRESS 21/150 Lat Phrao Rd, Chom Phon,
Chatuchak, Bangkok, 10900, Thailand